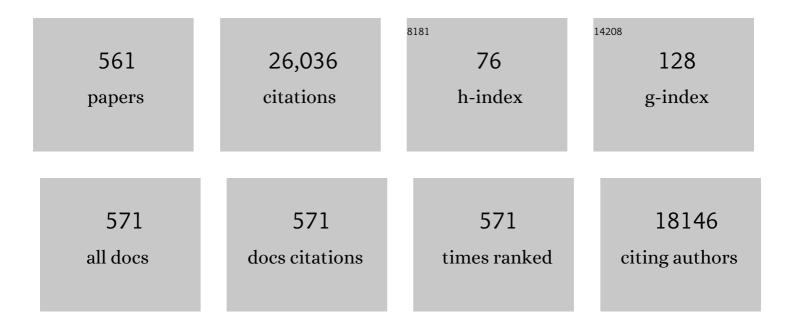
## Jeong Min Lee

List of Publications by Year in descending order

Source: https://exaly.com/author-pdf/7449861/publications.pdf Version: 2024-02-01



#	Article	IF	CITATIONS
1	Asia–Pacific clinical practice guidelines on the management of hepatocellular carcinoma: a 2017 update. Hepatology International, 2017, 11, 317-370.	4.2	1,537
2	Asian Pacific Association for the Study of the Liver consensus recommendations on hepatocellular carcinoma. Hepatology International, 2010, 4, 439-474.	4.2	944
3	Oncological Benefits of Neoadjuvant Chemoradiation With Gemcitabine Versus Upfront Surgery in Patients With Borderline Resectable Pancreatic Cancer. Annals of Surgery, 2018, 268, 215-222.	4.2	497
4	CT and MR Imaging Diagnosis and Staging of Hepatocellular Carcinoma: Part II. Extracellular Agents, Hepatobiliary Agents, and Ancillary Imaging Features. Radiology, 2014, 273, 30-50.	7.3	430
5	CT and MR Imaging Diagnosis and Staging of Hepatocellular Carcinoma: Part I. Development, Growth, and Spread: Key Pathologic and Imaging Aspects. Radiology, 2014, 272, 635-654.	7.3	401
6	Hepatocellular Carcinoma: Diagnostic Performance of Multidetector CT and MR Imaging—A Systematic Review and Meta-Analysis. Radiology, 2015, 275, 97-109.	7.3	393
7	Percutaneous Radiofrequency Ablation for Inoperable Non–Small Cell Lung Cancer and Metastases: Preliminary Report. Radiology, 2004, 230, 125-134.	7.3	332
8	Locally Advanced Rectal Cancer: Added Value of Diffusion-weighted MR Imaging in the Evaluation of Tumor Response to Neoadjuvant Chemo- and Radiation Therapy. Radiology, 2009, 253, 116-125.	7.3	325
9	Major Complications after Radio-frequency Thermal Ablation of Hepatic Tumors: Spectrum of Imaging Findings. Radiographics, 2003, 23, 123-134.	3.3	320
10	Imaging diagnosis of pancreatic cancer: A state-of-the-art review. World Journal of Gastroenterology, 2014, 20, 7864.	3.3	297
11	25 Years of Contrast-Enhanced MRI: Developments, Current Challenges and Future Perspectives. Advances in Therapy, 2016, 33, 1-28.	2.9	297
12	Radiofrequency Ablation of Hepatocellular Carcinoma as First-Line Treatment: Long-term Results and Prognostic Factors in 162 Patients with Cirrhosis. Radiology, 2014, 270, 900-909.	7.3	256
13	2018 Korean Liver Cancer Association–National Cancer Center Korea Practice Guidelines for the Management of Hepatocellular Carcinoma. Gut and Liver, 2019, 13, 227-299.	2.9	255
14	Small (â‰ <b>2</b> 0 mm) Pancreatic Adenocarcinomas: Analysis of Enhancement Patterns and Secondary Signs with Multiphasic Multidetector CT. Radiology, 2011, 259, 442-452.	7.3	212
15	Preoperative Assessment of Resectability of Hepatic Hilar Cholangiocarcinoma: Combined CT and Cholangiography with Revised Criteria. Radiology, 2006, 239, 113-121.	7.3	200
16	Intrahepatic Mass-forming Cholangiocarcinomas: Enhancement Patterns at Multiphasic CT, with Special Emphasis on Arterial Enhancement Pattern—Correlation with Clinicopathologic Findings. Radiology, 2011, 260, 148-157.	7.3	200
17	Gadoxetic Acid-Enhanced Magnetic Resonance Imaging for Differentiating Small Hepatocellular Carcinomas (≪ cm in Diameter) From Arterial Enhancing Pseudolesions. Investigative Radiology, 2010, 45, 96-103.	6.2	199
18	Effect of muscle mass on toxicity and survival in patients with colon cancer undergoing adjuvant chemotherapy. Supportive Care in Cancer, 2015, 23, 687-694.	2.2	178

#	Article	IF	CITATIONS
19	Intravoxel Incoherent Motion Diffusion-weighted MR Imaging of Hepatocellular Carcinoma: Correlation with Enhancement Degree and Histologic Grade. Radiology, 2014, 270, 758-767.	7.3	175
20	2014 Korean Liver Cancer Study Group-National Cancer Center Korea Practice Guideline for the Management of Hepatocellular Carcinoma. Korean Journal of Radiology, 2015, 16, 465.	3.4	168
21	Treatment Guidelines for Branch Duct Type Intraductal Papillary Mucinous Neoplasms of the Pancreas: When Can We Operate or Observe?. Annals of Surgical Oncology, 2008, 15, 199-205.	1.5	165
22	Apparent diffusion coefficient for evaluating tumour response to neoadjuvant chemoradiation therapy for locally advanced rectal cancer. European Radiology, 2011, 21, 987-995.	4.5	162
23	Intrahepatic Mass-forming Cholangiocarcinoma: Enhancement Patterns on Gadoxetic Acid–enhanced MR Images. Radiology, 2012, 264, 751-760.	7.3	162
24	Hepatocellular Carcinoma: Imaging Patterns on Gadoxetic Acid–enhanced MR Images and Their Value as an Imaging Biomarker. Radiology, 2013, 267, 776-786.	7.3	154
25	Comparison of international guidelines for noninvasive diagnosis of hepatocellular carcinoma: 2018 update. Clinical and Molecular Hepatology, 2019, 25, 245-263.	8.9	154
26	Preoperative Evaluation of Bile Duct Cancer: MRI Combined with MR Cholangiopancreatography Versus MDCT with Direct Cholangiography. American Journal of Roentgenology, 2008, 190, 396-405.	2.2	148
27	Hepatic Fibrosis: Prospective Comparison of MR Elastography and US Shear-Wave Elastography for Evaluation. Radiology, 2014, 273, 772-782.	7.3	147
28	Macrocystic Neoplasms of the Pancreas: CT Differentiation of Serous Oligocystic Adenoma from Mucinous Cystadenoma and Intraductal Papillary Mucinous Tumor. American Journal of Roentgenology, 2006, 187, 1192-1198.	2.2	146
29	Intravoxel Incoherent Motion Diffusion-weighted MR Imaging for Characterization of Focal Pancreatic Lesions. Radiology, 2014, 270, 444-453.	7.3	146
30	Imaging Diagnosis of Intrahepatic and Perihilar Cholangiocarcinoma: Recent Advances and Challenges. Radiology, 2018, 288, 7-13.	7.3	145
31	Preoperative evaluation of pancreatic cancer: Comparison of gadoliniumâ€enhanced dynamic MRI with MR cholangiopancreatography versus MDCT. Journal of Magnetic Resonance Imaging, 2009, 30, 586-595.	3.4	136
32	Differentiation of intraductal papillary mucinous neoplasms from other pancreatic cystic masses: Comparison of multirowâ€detector CT and MR imaging using ROC analysis. Journal of Magnetic Resonance Imaging, 2007, 26, 86-93.	3.4	132
33	Ectopic Pancreas: CT Findings with Emphasis on Differentiation from Small Gastrointestinal Stromal Tumor and Leiomyoma. Radiology, 2009, 252, 92-100.	7.3	131
34	Consensus report of the 2nd International Forum for Liver MRI. European Radiology, 2009, 19, 975-989.	4.5	125
35	Assessment of a Model-Based, Iterative Reconstruction Algorithm (MBIR) Regarding Image Quality and Dose Reduction in Liver Computed Tomography. Investigative Radiology, 2013, 48, 598-606.	6.2	119
36	Noninvasive diagnosis of hepatocellular carcinoma on gadoxetic acid-enhanced MRI: can hypointensity on the hepatobiliary phase be used as an alternative to washout?. European Radiology, 2015, 25, 2859-2868.	4.5	117

Jeong Min Lee

#	Article	IF	CITATIONS
37	Peripheral Mass–Forming Cholangiocarcinoma in Cirrhotic Liver. American Journal of Roentgenology, 2007, 189, 1428-1434.	2.2	114
38	Multiphasic MDCT Enhancement Pattern of Hepatocellular Carcinoma Smaller Than 3 cm in Diameter: Tumor Size and Cellular Differentiation. American Journal of Roentgenology, 2009, 193, W482-W489.	2.2	113
39	Hepatic Arterioportal Shunts: Dynamic CT and MR Features. Korean Journal of Radiology, 2002, 3, 1.	3.4	110
40	Hepatocellular Carcinoma in Patients with Chronic Liver Disease: Comparison of SPIO-enhanced MR Imaging and 16–Detector Row CT. Radiology, 2006, 238, 531-541.	7.3	109
41	Differentiating Malignant from Benign Common Bile Duct Stricture with Multiphasic Helical CT. Radiology, 2005, 236, 178-183.	7.3	107
42	Intrapancreatic Accessory Spleen: Findings on MR Imaging, CT, US and Scintigraphy, and the Pathologic Analysis. Korean Journal of Radiology, 2008, 9, 162.	3.4	107
43	Accuracy of Preoperative T-Staging of Gallbladder Carcinoma Using MDCT. American Journal of Roentgenology, 2008, 190, 74-80.	2.2	106
44	Small (â‰ <b>8</b> cm) Solid Pseudopapillary Tumors of the Pancreas at Multiphasic Multidetector CT. Radiology, 2010, 257, 97-106.	7.3	106
45	Hilar Cholangiocarcinoma: Role of Preoperative Imaging with Sonography, MDCT, MRI, and Direct Cholangiography. American Journal of Roentgenology, 2008, 191, 1448-1457.	2.2	103
46	Real-time US-CT/MR fusion imaging for percutaneous radiofrequency ablation of hepatocellular carcinoma. Journal of Hepatology, 2017, 66, 347-354.	3.7	103
47	Gadobenate dimeglumine-enhanced liver MR imaging: value of dynamic and delayed imaging for the characterization and detection of focal liver lesions. European Radiology, 2004, 14, 5-13.	4.5	102
48	MR Imaging-Histopathologic Correlation of Radiofrequency Thermal Ablation Lesion in a Rabbit Liver Model: Observation during Acute and Chronic Stages. Korean Journal of Radiology, 2001, 2, 151.	3.4	101
49	Esophageal Varices in Patients with Cirrhosis: Multidetector CT Esophagography—Comparison with Endoscopy. Radiology, 2007, 242, 759-768.	7.3	98
50	Analysis of Enhancement Pattern of Flat Gallbladder Wall Thickening on MDCT to Differentiate Gallbladder Cancer from Cholecystitis. American Journal of Roentgenology, 2008, 191, 765-771.	2.2	98
51	Prediction of microvascular invasion of hepatocellular carcinoma using gadoxetic acid-enhanced MR and 18F-FDG PET/CT. Abdominal Imaging, 2015, 40, 843-851.	2.0	98
52	Small Single-Nodule Hepatocellular Carcinoma: Comparison of Transarterial Chemoembolization, Radiofrequency Ablation, and Hepatic Resection by Using Inverse Probability Weighting. Radiology, 2014, 271, 909-918.	7.3	97
53	Prediction of Esophageal Varices in Patients with Cirrhosis: Usefulness of Three-dimensional MR Elastography with Echo-planar Imaging Technique. Radiology, 2014, 272, 143-153.	7.3	97
54	Magnetic resonance imaging findings of the massâ€forming type of autoimmune pancreatitis: Comparison with pancreatic adenocarcinoma. Journal of Magnetic Resonance Imaging, 2012, 36, 188-197.	3.4	95

#	Article	IF	CITATIONS
55	<b>Gastrointestinal Stromal Tumors of the Stomach:</b> CT Findings and Prediction of Malignancy. American Journal of Roentgenology, 2004, 183, 893-898.	2.2	93
56	MR elastography for noninvasive assessment of hepatic fibrosis: Reproducibility of the examination and reproducibility and repeatability of the liver stiffness value measurement. Journal of Magnetic Resonance Imaging, 2014, 39, 326-331.	3.4	93
57	Evaluation of hepatic focal lesions using diffusionâ€weighted MR imaging: Comparison of apparent diffusion coefficient and intravoxel incoherent motionâ€derived parameters. Journal of Magnetic Resonance Imaging, 2014, 39, 276-285.	3.4	93
58	Intussusception in Adults: From Stomach to Rectum. American Journal of Roentgenology, 2004, 183, 691-698.	2.2	92
59	Comparison of Gadobenate Dimeglumine-Enhanced Dynamic MRI and 16-MDCT for the Detection of Hepatocellular Carcinoma. American Journal of Roentgenology, 2006, 186, 149-157.	2.2	92
60	Attenuation-based Automatic Tube Voltage Selection and Tube Current Modulation for Dose Reduction at Contrast-enhanced Liver CT. Radiology, 2012, 265, 437-447.	7.3	92
61	Antiplatelet therapy and the risk of hepatocellular carcinoma in chronic hepatitis B patients on antiviral treatment. Hepatology, 2017, 66, 1556-1569.	7.3	92
62	Classification and prognosis of intrahepatic biliary stricture after liver transplantation. Liver Transplantation, 2007, 13, 1736-1742.	2.4	91
63	Progression of Pancreatic Branch Duct Intraductal Papillary Mucinous Neoplasm Associates With Cyst Size. Gastroenterology, 2018, 154, 576-584.	1.3	91
64	Combined hepatocellular cholangiocarcinoma: LI-RADS v2017 categorisation for differential diagnosis and prognostication on gadoxetic acid-enhanced MR imaging. European Radiology, 2019, 29, 373-382.	4.5	89
65	Enhancement patterns of hepatocellular carcinomas on multiphasic multidetector row CT: comparison with pathological differentiation. British Journal of Radiology, 2012, 85, e573-e583.	2.2	88
66	Pancreatic Steatosis and Fibrosis: Quantitative Assessment with Preoperative Multiparametric MR Imaging. Radiology, 2016, 279, 140-150.	7.3	88
67	MR elastography for noninvasive assessment of hepatic fibrosis: Experience from a tertiary center in asia. Journal of Magnetic Resonance Imaging, 2011, 34, 1110-1116.	3.4	86
68	Consensus report from the 7th International Forum for Liver Magnetic Resonance Imaging. European Radiology, 2016, 26, 674-682.	4.5	86
69	Safety Margin Assessment After Radiofrequency Ablation of the Liver Using Registration of Preprocedure and Postprocedure CT Images. American Journal of Roentgenology, 2011, 196, W565-W572.	2.2	85
70	Shear Wave Elastography for Liver Stiffness Measurement in Clinical Sonographic Examinations. Journal of Ultrasound in Medicine, 2014, 33, 437-447.	1.7	85
71	Detection of liver metastases: gadobenate dimeglumine-enhanced three-dimensional dynamic phases and one-hour delayed phase MR imaging versus superparamagnetic iron oxide-enhanced MR imaging. European Radiology, 2005, 15, 220-228.	4.5	84
72	Hepatocellular Carcinoma in Liver Transplantation Candidates: Detection with Gadobenate Dimeglumine–Enhanced MRI. American Journal of Roentgenology, 2008, 191, 529-536.	2.2	82

Jeong Min Lee

#	Article	IF	CITATIONS
73	Dual-Energy Computed Tomography to Assess Tumor Response to Hepatic Radiofrequency Ablation. Investigative Radiology, 2011, 46, 77-84.	6.2	82
74	Evaluation of Hepatic Fibrosis Using Intravoxel Incoherent Motion in Diffusion-Weighted Liver MRI. Journal of Computer Assisted Tomography, 2014, 38, 110-116.	0.9	82
75	MR elastography of healthy liver parenchyma: Normal value and reliability of the liver stiffness value measurement. Journal of Magnetic Resonance Imaging, 2013, 38, 1215-1223.	3.4	80
76	Intravoxel Incoherent Motion Diffusion-weighted MR Imaging for Monitoring the Therapeutic Efficacy of the Vascular Disrupting Agent CKD-516 in Rabbit VX2 Liver Tumors. Radiology, 2014, 272, 417-426.	7.3	80
77	<b>Primary and Secondary Lung Malignancies Treated with Percutaneous Radiofrequency Ablation:</b> Evaluation with Follow-Up Helical CT. American Journal of Roentgenology, 2004, 183, 1013-1020.	2.2	78
78	Diagnostic Performance of Gadoxetic Acid–enhanced Liver MR Imaging versus Multidetector CT in the Detection of Dysplastic Nodules and Early Hepatocellular Carcinoma. Radiology, 2017, 285, 134-146.	7.3	78
79	Nonhypervascular Pancreatic Neuroendocrine Tumors: Differential Diagnosis from Pancreatic Ductal Adenocarcinomas at MR Imaging—Retrospective Cross-sectional Study. Radiology, 2017, 284, 77-87.	7.3	77
80	Radio-frequency thermal ablation with hypertonic saline solution injection of the lung: ex vivo and in vivo feasibility studies. European Radiology, 2003, 13, 2540-2547.	4.5	76
81	MR Imaging Features of Small Solid Pseudopapillary Tumors: Retrospective Differentiation From Other Small Solid Pancreatic Tumors. American Journal of Roentgenology, 2010, 195, 1324-1332.	2.2	76
82	Retrospective validation of a new diagnostic criterion for hepatocellular carcinoma on gadoxetic acid-enhanced MRI: can hypointensity on the hepatobiliary phase be used as an alternative to washout with the aid of ancillary features?. European Radiology, 2019, 29, 1724-1732.	4.5	76
83	Contrastâ€enhanced MRI combined with MR cholangiopancreatography for the evaluation of patients with biliary strictures: Differentiation of malignant from benign bile duct strictures. Journal of Magnetic Resonance Imaging, 2007, 26, 304-312.	3.4	75
84	Solid Pancreatic Lesions: Characterization by Using Timing Bolus Dynamic Contrast-enhanced MR Imaging Assessment—A Preliminary Study. Radiology, 2013, 266, 185-196.	7.3	74
85	Preoperative Assessment of Pancreatic Cancer with FDG PET/MR Imaging versus FDG PET/CT Plus Contrast-enhanced Multidetector CT: A Prospective Preliminary Study. Radiology, 2017, 282, 149-159.	7.3	74
86	Image Fusion in Dual Energy Computed Tomography for Detection of Hypervascular Liver Hepatocellular Carcinoma. Investigative Radiology, 2010, 45, 149-157.	6.2	73
87	Differentiation of intrahepatic mass-forming cholangiocarcinoma from hepatocellular carcinoma on gadoxetic acid-enhanced liver MR imaging. European Radiology, 2016, 26, 1808-1817.	4.5	73
88	Prospective Evaluation of Hepatic Steatosis Using Ultrasound Attenuation Imaging in Patients with Chronic Liver Disease with Magnetic Resonance Imaging Proton Density Fat Fraction as the Reference Standard. Ultrasound in Medicine and Biology, 2019, 45, 1407-1416.	1.5	72
89	Hepatic Macrosteatosis: Predicting Appropriateness of Liver Donation by Using MR Imaging—Correlation with Histopathologic Findings. Radiology, 2006, 240, 116-129.	7.3	71
90	Pancreatic neuroendocrine tumour (PNET): Staging accuracy of MDCT and its diagnostic performance for the differentiation of PNET with uncommon CT findings from pancreatic adenocarcinoma. European Radiology, 2016, 26, 1338-1347.	4.5	71

#	Article	IF	CITATIONS
91	Appropriateness of a Donor Liver with Respect to Macrosteatosis: Application of Artificial Neural Networks to US Images—Initial Experience. Radiology, 2005, 234, 793-803.	7.3	70
92	Quantitative CT Color Mapping of the Arterial Enhancement Fraction of the Liver to Detect Hepatocellular Carcinoma. Radiology, 2009, 250, 425-4s34.	7.3	70
93	Non-hypervascular hepatobiliary phase hypointense nodules on gadoxetic acid-enhanced MRI: Risk of HCC recurrence after radiofrequency ablation. Journal of Hepatology, 2015, 62, 1122-1130.	3.7	70
94	Estimation of Hepatic Extracellular Volume Fraction Using Multiphasic Liver Computed Tomography for Hepatic Fibrosis Grading. Investigative Radiology, 2015, 50, 290-296.	6.2	70
95	Quantitative assessment of hepatic function: modified look-locker inversion recovery (MOLLI) sequence for T1 mapping on Gd-EOB-DTPA-enhanced liver MR imaging. European Radiology, 2016, 26, 1775-1782.	4.5	69
96	Feasibility and Accuracy of Dual-Source Dual-Energy CT for Noninvasive Determination of Hepatic Iron Accumulation. Radiology, 2012, 262, 126-135.	7.3	68
97	Recent Advances in the Imaging Diagnosis of Hepatocellular Carcinoma: Value of Gadoxetic Acid-Enhanced MRI. Liver Cancer, 2016, 5, 67-87.	7.7	68
98	The Value of Gadobenate Dimeglumine-Enhanced Delayed Phase MR Imaging for Characterization of Hepatocellular Nodules in the Cirrhotic Liver. Investigative Radiology, 2008, 43, 202-210.	6.2	67
99	Diagnostic Performance of 64-Channel Multidetector CT in the Evaluation of Gastric Cancer: Differentiation of Mucosal Cancer (T1a) from Submucosal Involvement (T1b and T2). Radiology, 2010, 255, 805-814.	7.3	67
100	Staging of Hepatic Fibrosis: Comparison of Magnetic Resonance Elastography and Shear Wave Elastography in the Same Individuals. Korean Journal of Radiology, 2013, 14, 202.	3.4	67
101	Diagnostic accuracy of liver imaging reporting and data system (Llâ€RADS) v2014 for intrahepatic massâ€forming cholangiocarcinomas in patients with chronic liver disease on gadoxetic acidâ€enhanced MRI. Journal of Magnetic Resonance Imaging, 2016, 44, 1330-1338.	3.4	67
102	Clinical Feasibility of 3-Dimensional Magnetic Resonance Cholangiopancreatography Using Compressed Sensing. Investigative Radiology, 2017, 52, 612-619.	6.2	66
103	Quantitative Liver Function Analysis: Volumetric T1 Mapping with Fast Multisection B <sub>1</sub> Inhomogeneity Correction in Hepatocyte-specific Contrast-enhanced Liver MR Imaging. Radiology, 2017, 282, 408-417.	7.3	65
104	Dynamic contrast-enhanced MRI to evaluate the therapeutic response to neoadjuvant chemoradiation therapy in locally advanced rectal cancer. Journal of Magnetic Resonance Imaging, 2014, 40, 730-737.	3.4	64
105	Prospective comparison of 3T MRI with diffusionâ€weighted imaging and MDCT for the preoperative TNM staging of gastric cancer. Journal of Magnetic Resonance Imaging, 2015, 41, 814-821.	3.4	64
106	Added Value of Integrated Whole-Body PET/MRI for Evaluation of Colorectal Cancer: Comparison With Contrast-Enhanced MDCT. American Journal of Roentgenology, 2016, 206, W10-W20.	2.2	64
107	MRI Features of Gastrointestinal Stromal Tumors. American Journal of Roentgenology, 2014, 203, 980-991.	2.2	63
108	MDCT and superparamagnetic iron oxide (SPIO)-enhanced MR findings of intrapancreatic accessory spleen in seven patients. European Radiology, 2006, 16, 1887-1897.	4.5	62

#	Article	IF	CITATIONS
109	Recent Advances in CT and MR Imaging for Evaluation of Hepatocellular Carcinoma. Liver Cancer, 2012, 1, 22-40.	7.7	62
110	Accuracy of MRI for predicting the circumferential resection margin, mesorectal fascia invasion, and tumor response to neoadjuvant chemoradiotherapy for locally advanced rectal cancer. Journal of Magnetic Resonance Imaging, 2009, 29, 1093-1101.	3.4	61
111	Diagnosis of Hepatocellular Carcinoma: Newer Radiological Tools. Seminars in Oncology, 2012, 39, 399-409.	2.2	61
112	2014 KLCSG-NCC Korea Practice Guidelines for the Management of Hepatocellular Carcinoma: HCC Diagnostic Algorithm. Digestive Diseases, 2014, 32, 764-777.	1.9	60
113	Hepatic Steatosis: Assessment with Acoustic Structure Quantification of US Imaging. Radiology, 2016, 278, 257-264.	7.3	60
114	Quantitative Assessment of Liver Function by Using Gadoxetic Acid–enhanced MRI: Hepatocyte Uptake Ratio. Radiology, 2019, 290, 125-133.	7.3	59
115	Colorectal Cancer Liver Metastases: Diagnostic Performance and Prognostic Value of PET/MR Imaging. Radiology, 2016, 280, 782-792.	7.3	58
116	Consensus Report of the 4th International Forum for Gadolinium-Ethoxybenzyl-Diethylenetriamine Pentaacetic Acid Magnetic Resonance Imaging. Korean Journal of Radiology, 2011, 12, 403.	3.4	57
117	Percutaneous Radiofrequency Ablation with Multiple Electrodes for Medium-Sized Hepatocellular Carcinomas. Korean Journal of Radiology, 2012, 13, 34.	3.4	57
118	Added value of diffusionâ€weighted imaging to MR cholangiopancreatography with unenhanced mr imaging for predicting malignancy or invasiveness of intraductal papillary mucinous neoplasm of the pancreas. Journal of Magnetic Resonance Imaging, 2013, 38, 555-563.	3.4	57
119	Nonalcoholic Fatty Liver Disease: Intravoxel Incoherent Motion Diffusion-weighted MR Imaging—An Experimental Study in a Rabbit Model. Radiology, 2014, 270, 131-140.	7.3	57
120	A Comparative Experimental Study of the In-vitro Efficiency of Hypertonic Saline-Enhanced Hepatic Bipolar and Monopolar Radiofrequency Ablation. Korean Journal of Radiology, 2003, 4, 163.	3.4	56
121	A prospective randomized study comparing radiofrequency ablation and hepatic resection for hepatocellular carcinoma. Annals of Surgical Treatment and Research, 2018, 94, 74.	1.0	56
122	State-of-the-art preoperative staging of gastric cancer by MDCT and magnetic resonance imaging. World Journal of Gastroenterology, 2014, 20, 4546.	3.3	56
123	Switching Monopolar Radiofrequency Ablation Technique Using Multiple, Internally Cooled Electrodes and a Multichannel Generator. Investigative Radiology, 2007, 42, 163-171.	6.2	55
124	Dual-source, dual-energy multidetector CT for the evaluation of pancreatic tumours. British Journal of Radiology, 2012, 85, e891-e898.	2.2	55
125	Low Tube Voltage Intermediate Tube Current Liver MDCT: Sinogram-Affirmed Iterative Reconstruction Algorithm for Detection of Hypervascular Hepatocellular Carcinoma. American Journal of Roentgenology, 2013, 201, 23-32.	2.2	55
126	Liver imaging reporting and data system v2014 categorization of hepatocellular carcinoma on gadoxetic acidâ€enhanced MRI: Comparison with multiphasic multidetector computed tomography. Journal of Magnetic Resonance Imaging, 2017, 45, 731-740.	3.4	55

#	Article	IF	CITATIONS
127	LI-RADS Version 2017 versus Version 2018: Diagnosis of Hepatocellular Carcinoma on Gadoxetate Disodium–enhanced MRI. Radiology, 2019, 292, 655-663.	7.3	55
128	Consensus report from the 8th International Forum for Liver Magnetic Resonance Imaging. European Radiology, 2020, 30, 370-382.	4.5	55
129	High-grade Neuroendocrine Carcinomas of the Gallbladder and Bile Duct. Journal of Computer Assisted Tomography, 2006, 30, 604-609.	0.9	54
130	Focal Peliosis Hepatis as a Mimicker of Hepatic Tumors. Journal of Computer Assisted Tomography, 2007, 31, 79-85.	0.9	54
131	Acoustic Radiation Force Impulse Elastography for Chronic Liver Disease: Comparison with Ultrasound-Based Scores of Experienced Radiologists, Child-Pugh Scores and Liver Function Tests. Ultrasound in Medicine and Biology, 2010, 36, 1637-1643.	1.5	54
132	Gadoxetate Disodium–Enhanced Hepatobiliary Phase MRI of Hepatocellular Carcinoma: Correlation With Histological Characteristics. American Journal of Roentgenology, 2011, 197, 399-405.	2.2	54
133	Clinical application of controlled aliasing in parallel imaging results in a higher acceleration (CAIPIRINHA)â€volumetric interpolated breathhold (VIBE) sequence for gadoxetic acidâ€enhanced liver MR imaging. Journal of Magnetic Resonance Imaging, 2013, 38, 1020-1026.	3.4	54
134	Liver Fibrosis Staging with MR Elastography: Comparison of Diagnostic Performance between Patients with Chronic Hepatitis B and Those with Other Etiologic Causes. Radiology, 2016, 280, 88-97.	7.3	54
135	Assessment of Malignant Potential in Intraductal Papillary Mucinous Neoplasms of the Pancreas: Comparison between Multidetector CT and MR Imaging with MR Cholangiopancreatography. Radiology, 2016, 279, 128-139.	7.3	54
136	Value of Contrast-Enhanced Sonography for the Characterization of Focal Hepatic Lesions in Patients with Diffuse Liver Disease: Receiver Operating Characteristic Analysis. American Journal of Roentgenology, 2005, 184, 1077-1084.	2.2	53
137	Usefulness of CT volumetry for primary gastric lesions in predicting pathologic response to neoadjuvant chemotherapy in advanced gastric cancer. Abdominal Imaging, 2009, 34, 430-440.	2.0	53
138	Advancement in HCC imaging: diagnosis, staging and treatment efficacy assessments. Journal of Hepato-Biliary-Pancreatic Sciences, 2010, 17, 369-373.	2.6	53
139	Hepatocellular nodules in liver cirrhosis: MR evaluation. Abdominal Imaging, 2011, 36, 282-289.	2.0	53
140	MR Imaging in Patients with Suspected Liver Metastases: Value of Liver-Specific Contrast Agent Gadoxetic Acid. Korean Journal of Radiology, 2013, 14, 894.	3.4	53
141	Recent Advances in the Image-Guided Tumor Ablation of Liver Malignancies: Radiofrequency Ablation with Multiple Electrodes, Real-Time Multimodality Fusion Imaging, and New Energy Sources. Korean Journal of Radiology, 2018, 19, 545.	3.4	53
142	Assessment of the treatment response of HCC. Abdominal Imaging, 2011, 36, 300-314.	2.0	52
143	Free-breathing dynamic contrast-enhanced MRI of the abdomen and chest using a radial gradient echo sequence with K-space weighted image contrast (KWIC). European Radiology, 2013, 23, 1352-1360.	4.5	52
144	Primary malignant tumours in the non-cirrhotic liver. European Journal of Radiology, 2017, 95, 349-361.	2.6	52

#	Article	IF	CITATIONS
145	Two- versus Three-dimensional Colon Evaluation with Recently Developed Virtual Dissection Software for CT Colonography. Radiology, 2007, 244, 852-864.	7.3	51
146	Imaging bile duct tumors: pathologic concepts, classification, and early tumor detection. Abdominal Imaging, 2013, 38, 1334-1350.	2.0	51
147	Small- and Medium-sized Hepatocellular Carcinomas: Monopolar Radiofrequency Ablation with a Multiple-Electrode Switching System—Mid-term Results. Radiology, 2013, 268, 589-600.	7.3	51
148	Reproducibility of ultrasound attenuation imaging for the noninvasive evaluation of hepatic steatosis. Ultrasonography, 2020, 39, 121-129.	2.3	51
149	Gadobenate Dimeglumine-Enhanced Liver MRI as the Sole Preoperative Imaging Technique: A Prospective Study of Living Liver Donors. American Journal of Roentgenology, 2006, 187, 1223-1233.	2.2	50
150	Hepatic Steatosis in Living Liver Donor Candidates: Preoperative Assessment by Using Breath-hold Triple-Echo MR Imaging and <sup>1</sup> H MR Spectroscopy. Radiology, 2014, 271, 730-738.	7.3	50
151	Reduced Field-of-View Diffusion-Weighted Magnetic Resonance Imaging of the Pancreas: Comparison with Conventional Single-Shot Echo-Planar Imaging. Korean Journal of Radiology, 2015, 16, 1216.	3.4	50
152	Rapid Imaging: Recent Advances in Abdominal MRI for Reducing Acquisition Time and Its Clinical Applications. Korean Journal of Radiology, 2019, 20, 1597.	3.4	50
153	CT-guided celiac plexus block for intractable abdominal pain. Journal of Korean Medical Science, 2000, 15, 173.	2.5	48
154	Primary Gastrointestinal Stromal Tumors in the Omentum and Mesentery: CT Findings and Pathologic Correlations. American Journal of Roentgenology, 2004, 182, 1463-1467.	2.2	48
155	Diagnostic Accuracy of Multi-/Single-Detector Row CT and Contrast-Enhanced MRI in the Detection of Hepatocellular Carcinomas Meeting the Milan Criteria before Liver Transplantation. Intervirology, 2008, 51, 52-60.	2.8	48
156	Intravoxel Incoherent Motion Diffusion-Weighted Imaging of Pancreatic Neuroendocrine Tumors. Investigative Radiology, 2014, 49, 396-402.	6.2	48
157	Noninvasive Diagnosis of Hepatocellular Carcinoma: Elaboration on Korean Liver Cancer Study Group-National Cancer Center Korea Practice Guidelines Compared with Other Guidelines and Remaining Issues. Korean Journal of Radiology, 2016, 17, 7.	3.4	48
158	Multiple-Electrode Radiofrequency Ablation of In Vivo Porcine Liver. Investigative Radiology, 2007, 42, 676-683.	6.2	46
159	Gadoxetic acid disodiumâ€enhanced magnetic resonance imaging for biliary and vascular evaluations in preoperative living liver donors: Comparison with gadobenate dimeglumineâ€enhanced MRI. Journal of Magnetic Resonance Imaging, 2011, 33, 149-159.	3.4	46
160	Preoperative CT Classification of the Resectability of Pancreatic Cancer: Interobserver Agreement. Radiology, 2019, 293, 343-349.	7.3	46
161	Preoperative evaluation of the hepatic vascular anatomy in living liver donors: Comparison of CT angiography and MR angiography. Journal of Magnetic Resonance Imaging, 2006, 24, 1081-1087.	3.4	45
162	Comparison of Magnetic Resonance Elastography and Gadoxetate Disodium–Enhanced Magnetic Resonance Imaging for the Evaluation of Hepatic Fibrosis. Investigative Radiology, 2013, 48, 607-613.	6.2	45

#	Article	IF	CITATIONS
163	Threeâ€dimensional dynamic liver MR imaging using sensitivity encoding for detection of hepatocellular carcinomas: Comparison with superparamagnetic iron oxideâ€enhanced MR imaging. Journal of Magnetic Resonance Imaging, 2004, 20, 826-837.	3.4	44
164	Two-way actuation behavior of shape memory polymer/elastomer core/shell composites. Smart Materials and Structures, 2012, 21, 035028.	3.5	44
165	80-kVp CT Using Iterative Reconstruction in Image Space Algorithm for the Detection of Hypervascular Hepatocellular Carcinoma: Phantom and Initial Clinical Experience. Korean Journal of Radiology, 2012, 13, 152.	3.4	44
166	Integrated Whole Body MR/PET: Where Are We?. Korean Journal of Radiology, 2015, 16, 32.	3.4	44
167	Combined Use of MR Fat Quantification and MR Elastography in Living Liver Donors: Can It Reduce the Need for Preoperative Liver Biopsy?. Radiology, 2015, 276, 453-464.	7.3	44
168	Comparison of Superparamagnetic Iron Oxide–Enhanced and Gadobenate Dimeglumine–Enhanced Dynamic MRI for Detection of Small Hepatocellular Carcinomas. American Journal of Roentgenology, 2004, 182, 1217-1223.	2.2	43
169	Superparamagnetic Iron Oxide-Enhanced Liver Magnetic Resonance Imaging. Investigative Radiology, 2006, 41, 168-174.	6.2	43
170	CT Differentiation of Cholangiocarcinoma from Periductal Fibrosis in Patients with Hepatolithiasis. American Journal of Roentgenology, 2006, 187, 445-453.	2.2	43
171	Adaptive Statistical Iterative Reconstruction and Veo. Journal of Computer Assisted Tomography, 2012, 36, 596-601.	0.9	43
172	Hepatocellular Carcinoma: Texture Analysis of Preoperative Computed Tomography Images Can Provide Markers of Tumor Grade and Disease-Free Survival. Korean Journal of Radiology, 2019, 20, 569.	3.4	43
173	Contrastâ€Enhanced Agent Detection Imaging. Journal of Ultrasound in Medicine, 2003, 22, 897-910.	1.7	42
174	Contrast-Enhanced Sonography of Intrapancreatic Accessory Spleen in Six Patients. American Journal of Roentgenology, 2007, 188, 422-428.	2.2	42
175	Changes of Portosystemic Collaterals and Splenic Volume on CT After Liver Transplantation and Factors Influencing Those Changes. American Journal of Roentgenology, 2008, 191, W8-W16.	2.2	42
176	Imaging diagnosis and staging of hepatocellular carcinoma. Liver Transplantation, 2011, 17, S34-S43.	2.4	42
177	Quantitative Color Mapping of the Arterial Enhancement Fraction in Patients With Diffuse Liver Disease. American Journal of Roentgenology, 2011, 197, 876-883.	2.2	42
178	Quantification of the Fat Fraction in the Liver Using Dual-Energy Computed Tomography and Multimaterial Decomposition. Journal of Computer Assisted Tomography, 2014, 38, 845-852.	0.9	42
179	Diagnosis of Hepatocellular Carcinoma with Gadoxetic Acid-Enhanced MRI: 2016 Consensus Recommendations of the Korean Society of Abdominal Radiology. Korean Journal of Radiology, 2017, 18, 427.	3.4	42
180	Magnetic resonance with diffusion-weighted imaging improves assessment of focal liver lesions in patients with potentially resectable pancreatic cancer on CT. European Radiology, 2018, 28, 3484-3493.	4.5	42

#	Article	IF	CITATIONS
181	Radiologic-Pathologic Correlation of Hepatobiliary Phase Hypointense Nodules without Arterial Phase Hyperenhancement at Gadoxetic Acid–enhanced MRI: A Multicenter Study. Radiology, 2020, 296, 335-345.	7.3	42
182	Optimal interventional treatment and longâ€ŧerm outcomes for biliary stricture after liver transplantation. Clinical Transplantation, 2008, 22, 484-493.	1.6	41
183	Differentiation of Intraductal Growing–type Cholangiocarcinomas from Nodular-type Cholangiocarcinomas at Biliary MR Imaging with MR Cholangiography. Radiology, 2010, 257, 364-372.	7.3	41
184	Diagnostic Performance of Gadoxetic Acid–enhanced Liver MR Imaging in the Detection of HCCs and Allocation of Transplant Recipients on the Basis of the Milan Criteria and UNOS Guidelines: Correlation with Histopathologic Findings. Radiology, 2015, 274, 149-160.	7.3	41
185	Pre-treatment estimation of future remnant liver function using gadoxetic acid MRI in patients with HCC. Journal of Hepatology, 2016, 65, 1155-1162.	3.7	41
186	Hepatic stiffness measurement by using MR elastography: prognostic values after hepatic resection for hepatocellular carcinoma. European Radiology, 2017, 27, 1713-1721.	4.5	41
187	Evaluation of Transient Motion During Gadoxetic Acid–Enhanced Multiphasic Liver Magnetic Resonance Imaging Using Free-Breathing Golden-Angle Radial Sparse Parallel Magnetic Resonance Imaging. Investigative Radiology, 2018, 53, 52-61.	6.2	41
188	Outcome of No-Touch Radiofrequency Ablation for Small Hepatocellular Carcinoma: A Multicenter Clinical Trial. Radiology, 2021, 301, 229-236.	7.3	41
189	MRI Findings of Focal Eosinophilic Liver Diseases. American Journal of Roentgenology, 2005, 184, 1541-1548.	2.2	40
190	Consensus report from the 6th International forum for liver MRI using gadoxetic acid. Journal of Magnetic Resonance Imaging, 2014, 40, 516-529.	3.4	40
191	A Comparison of Biannual Two-Phase Low-Dose Liver CT and US for HCC Surveillance in a Group at High Risk of HCC Development. Liver Cancer, 2020, 9, 503-517.	7.7	40
192	Navigatorâ€ŧriggered isotropic threeâ€dimensional magnetic resonance cholangiopancreatography in the diagnosis of malignant biliary obstructions: Comparison with direct cholangiography. Journal of Magnetic Resonance Imaging, 2008, 27, 94-101.	3.4	39
193	Gadobutrol-enhanced, Three-Dimensional, Dynamic MR Imaging With MR Cholangiography for the Preoperative Evaluation of Bile Duct Cancer. Investigative Radiology, 2010, 45, 217-224.	6.2	39
194	Role of diffusion-weighted magnetic resonance imaging in the diagnosis of gallbladder cancer. Journal of Magnetic Resonance Imaging, 2013, 38, 127-137.	3.4	39
195	Prediction of aggressiveness in early-stage hepatocellular carcinoma for selection of surgical resection. Journal of Hepatology, 2014, 60, 1219-1224.	3.7	39
196	Intraductal Papillary Mucinous Neoplasms of the Pancreas: Evaluation of Malignant Potential and Surgical Resectability by Using MR Imaging with MR Cholangiography. Radiology, 2015, 274, 723-733.	7.3	39
197	Diagnostic Accuracy of 3.0-Tesla Rectal Magnetic Resonance Imaging in Preoperative Local Staging of Primary Rectal Cancer. Investigative Radiology, 2008, 43, 587-593.	6.2	38
198	Evaluation of the Gross Type and Longitudinal Extent of Extrahepatic Cholangiocarcinomas on Contrast-Enhanced Multidetector Row Computed Tomography. Journal of Computer Assisted Tomography, 2009, 33, 376-382.	0.9	38

#	Article	IF	CITATIONS
199	Consensus Report of the Fifth International Forum for Liver MRI. American Journal of Roentgenology, 2013, 201, 97-107.	2.2	38
200	Diagnosing Borderline Hepatic Nodules in Hepatocarcinogenesis: Imaging Performance. American Journal of Roentgenology, 2015, 205, 10-21.	2.2	38
201	Laparoscopic Liver Resection versus Percutaneous Radiofrequency Ablation for Small Single Nodular Hepatocellular Carcinoma: Comparison of Treatment Outcomes. Liver Cancer, 2021, 10, 25-37.	7.7	38
202	Acute Cerebral Infarction After Radiofrequency Ablation of an Atypical Carcinoid Pulmonary Tumor. American Journal of Roentgenology, 2004, 182, 990-992.	2.2	37
203	Diagnostic Performance of Multidetector Row Computed Tomography, Superparamagnetic Iron Oxide-Enhanced Magnetic Resonance Imaging, and Dual-Contrast Magnetic Resonance Imaging in Predicting the Appropriateness of a Transplant Recipient Based on Milan Criteria. Investigative Radiology, 2009, 44, 311-321.	6.2	37
204	Cancer Stem Cells in Primary Liver Cancers: Pathological Concepts and Imaging Findings. Korean Journal of Radiology, 2015, 16, 50.	3.4	37
205	Monitoring Vascular Disrupting Therapy in a Rabbit Liver Tumor Model: Relationship between Tumor Perfusion Parameters at IVIM Diffusion-weighted MR Imaging and Those at Dynamic Contrast-enhanced MR Imaging. Radiology, 2016, 278, 104-113.	7.3	37
206	LI-RADS treatment response categorization on gadoxetic acid-enhanced MRI: diagnostic performance compared to mRECIST and added value of ancillary features. European Radiology, 2020, 30, 2861-2870.	4.5	37
207	CT findings of extramedullary hematopoiesis in the thorax, liver and kidneys, in a patient with idiopathic myelofibrosis. Journal of Korean Medical Science, 2000, 15, 460.	2.5	36
208	Percutaneous Radiofrequency Thermal Ablation of Lung VX2 Tumors in a Rabbit Model Using a Cooled Tip-Electrode. Investigative Radiology, 2003, 38, 129-139.	6.2	36
209	Diffusion-Related MRI Parameters for Assessing Early Treatment Response of Liver Metastases to Cytotoxic Therapy in Colorectal Cancer. American Journal of Roentgenology, 2016, 207, W26-W32.	2.2	36
210	Atypical Appearance of Hepatocellular Carcinoma and Its Mimickers: How to Solve Challenging Cases Using Gadoxetic Acid-Enhanced Liver Magnetic Resonance Imaging. Korean Journal of Radiology, 2019, 20, 1019.	3.4	36
211	Man or machine? Prospective comparison of the version 2018 EASL, LI-RADS criteria and a radiomics model to diagnose hepatocellular carcinoma. Cancer Imaging, 2019, 19, 84.	2.8	36
212	Contrast-enhanced ultrasound approach to the diagnosis of focal liver lesions: the importance of washout. Ultrasonography, 2019, 38, 289-301.	2.3	36
213	Percutaneous Radiofrequency Thermal Ablation with Hypertonic Saline Injection: In Vivo Study in a Rabbit Liver Model. Korean Journal of Radiology, 2003, 4, 27.	3.4	35
214	Imaging of Gastrointestinal Stromal Tumors. Journal of Computer Assisted Tomography, 2004, 28, 596-604.	0.9	35
215	Biliary Complications in Living Donor Liver Transplantation: Imaging Findings and the Roles of Interventional Procedures. CardioVascular and Interventional Radiology, 2005, 28, 756-767.	2.0	35
216	CT Features of an Intraductal Polypoid Mass. Journal of Computer Assisted Tomography, 2006, 30, 173-181.	0.9	35

#	Article	IF	CITATIONS
217	Hepatocellular Carcinoma in Cirrhotic Liver: Double-Contrast-Enhanced, High-Resolution 3.0T-MR Imaging With Pathologic Correlation. Investigative Radiology, 2008, 43, 538-546.	6.2	35
218	Adaptive Iterative Dose Reduction Algorithm in CT: Effect on Image Quality Compared with Filtered Back Projection in Body Phantoms of Different Sizes. Korean Journal of Radiology, 2014, 15, 195.	3.4	35
219	Portal Vein Thrombosis in Patients with Hepatocellular Carcinoma: Diagnostic Accuracy of Gadoxetic Acid–enhanced MR Imaging. Radiology, 2016, 279, 773-783.	7.3	35
220	Diagnostic Performance of LI-RADS Treatment Response Algorithm for Hepatocellular Carcinoma: Adding Ancillary Features to MRI Compared with Enhancement Patterns at CT and MRI. Radiology, 2020, 296, 554-561.	7.3	35
221	Comparison of Wet Radiofrequency Ablation with Dry Radiofrequency Ablation and Radiofrequency Ablation Using Hypertonic Saline Preinjection: Ex Vivo Bovine Liver. Korean Journal of Radiology, 2004, 5, 258.	3.4	34
222	Initial Assessment of Dual-Energy CT in Patients With Gallstones or Bile Duct Stones: Can Virtual Nonenhanced Images Replace True Nonenhanced Images?. American Journal of Roentgenology, 2012, 198, 817-824.	2.2	34
223	Open radio-frequency thermal ablation of renal VX2 tumors in a rabbit model using a cooled-tip electrode: feasibility, safety, and effectiveness. European Radiology, 2003, 13, 1324-1332.	4.5	33
224	Effect of Adjusted Positioning on Gastric Distention and Fluid Distribution During CT Gastrography. American Journal of Roentgenology, 2005, 185, 1180-1184.	2.2	33
225	Sonography Transmission Gel as Endorectal Contrast Agent for Tumor Visualization in Rectal Cancer. American Journal of Roentgenology, 2008, 191, 186-189.	2.2	33
226	Nucleos(t)ide Analogue Treatment for Patients With Hepatitis B Virus (HBV) e Antigen–Positive Chronic HBV Genotype C Infection: A Nationwide, Multicenter, Retrospective Study. Journal of Infectious Diseases, 2017, 216, 1407-1414.	4.0	33
227	MRI for Detection of Hepatocellular Carcinoma: Comparison of Mangafodipir Trisodium and Gadopentetate Dimeglumine Contrast Agents. American Journal of Roentgenology, 2004, 183, 1049-1054.	2.2	32
228	Differential CT Features of Intraductal Biliary Metastasis and Double Primary Intraductal Polypoid Cholangiocarcinoma in Patients With a History of Extrabiliary Malignancy. American Journal of Roentgenology, 2009, 193, 1061-1069.	2.2	32
229	Usefulness of MR elastography for predicting esophageal varices in cirrhotic patients. Journal of Magnetic Resonance Imaging, 2014, 39, 559-566.	3.4	32
230	Postablation Assessment Using Follow-Up Registration of CT Images Before and After Radiofrequency Ablation (RFA): Prospective Evaluation of Midterm Therapeutic Results of RFA for Hepatocellular Carcinoma. American Journal of Roentgenology, 2014, 203, 70-77.	2.2	32
231	GRASE Revisited: breath-hold three-dimensional (3D) magnetic resonance cholangiopancreatography using a Gradient and Spin Echo (GRASE) technique at 3T. European Radiology, 2018, 28, 3721-3728.	4.5	32
232	High Acceleration Three-Dimensional T1-Weighted Dual Echo Dixon Hepatobiliary Phase Imaging Using Compressed Sensing-Sensitivity Encoding: Comparison of Image Quality and Solid Lesion Detectability with the Standard T1-Weighted Sequence. Korean Journal of Radiology, 2019, 20, 438.	3.4	32
233	Contrast-enhanced US with Sulfur Hexafluoride and Perfluorobutane for the Diagnosis of Hepatocellular Carcinoma in Individuals with High Risk. Radiology, 2020, 297, 108-116.	7.3	32
234	Quantitative Ultrasound Radiofrequency Data Analysis for the Assessment of Hepatic Steatosis in Nonalcoholic Fatty Liver Disease Using Magnetic Resonance Imaging Proton Density Fat Fraction as the Reference Standard. Korean Journal of Radiology, 2021, 22, 1077.	3.4	32

#	Article	IF	CITATIONS
235	CT/MRI and CEUS LI-RADS Major Features Association with Hepatocellular Carcinoma: Individual Patient Data Meta-Analysis. Radiology, 2022, 302, 326-335.	7.3	32
236	Bipolar Radiofrequency Ablation Using Wet-Cooled Electrodes: An In Vitro Experimental Study in Bovine Liver. American Journal of Roentgenology, 2005, 184, 391-397.	2.2	31
237	MRI Features of Pancreatic Colloid Carcinoma. American Journal of Roentgenology, 2009, 193, W308-W313.	2.2	31
238	Noninvasive Assessment of Hepatic Fibrosis in Patients with Chronic Hepatitis B Viral Infection Using Magnetic Resonance Elastography. Korean Journal of Radiology, 2014, 15, 210.	3.4	31
239	Whole-body PET/MRI for colorectal cancer staging: Is it the way forward?. Journal of Magnetic Resonance Imaging, 2017, 45, 21-35.	3.4	31
240	Liver fibrosis staging with a new 2D-shear wave elastography using comb-push technique: Applicability, reproducibility, and diagnostic performance. PLoS ONE, 2017, 12, e0177264.	2.5	31
241	Focal Nodular Hyperplasia After Treatment With Oxaliplatin: A Multiinstitutional Series of Cases Diagnosed at MRI. American Journal of Roentgenology, 2018, 210, 775-779.	2.2	31
242	Initial M Staging of Rectal Cancer: FDG PET/MRI with a Hepatocyte-specific Contrast Agent versus Contrast-enhanced CT. Radiology, 2020, 294, 310-319.	7.3	31
243	Therapeutic Response Evaluation of Malignant Hepatic Masses Treated by Interventional Procedures With Contrastâ€Enhanced Agent Detection Imaging. Journal of Ultrasound in Medicine, 2003, 22, 911-920.	1.7	30
244	Detection of Small Hypervascular Hepatocellular Carcinomas in Cirrhotic Patients: Comparison of Superparamagnetic Iron Oxide-Enhanced MR Imaging with Dual-Phase Spiral CT. Korean Journal of Radiology, 2003, 4, 1.	3.4	30
245	Ex Vivo Experiment of Saline-Enhanced Hepatic Bipolar Radiofrequency Ablation with a Perfused Needle Electrode: Comparison with Conventional Monopolar and Simultaneous Monopolar Modes. CardioVascular and Interventional Radiology, 2005, 28, 338-345.	2.0	30
246	Radiofrequency Ablation of the Porcine Liver In Vivo: Increased Coagulation with an Internally Cooled Perfusion Electrode. Academic Radiology, 2006, 13, 343-352.	2.5	30
247	Computer-Aided Detection of Colonic Polyps at CT Colonography Using a Hessian Matrix–Based Algorithm: Preliminary Study. American Journal of Roentgenology, 2007, 189, 41-51.	2.2	30
248	Enhancement characteristics of cholangiocarcinomas on mutiphasic helical CT: emphasis on morphologic subtypes. Clinical Imaging, 2008, 32, 114-120.	1.5	30
249	The Right Posterior Bile Duct Anatomy of the Donor Is Important in Biliary Complications of the Recipients After Living-Donor Liver Transplantation. Annals of Surgery, 2013, 257, 702-707.	4.2	30
250	Comparison of biannual ultrasonography and annual non-contrast liver magnetic resonance imaging as surveillance tools for hepatocellular carcinoma in patients with liver cirrhosis (MAGNUS-HCC): a study protocol. BMC Cancer, 2017, 17, 877.	2.6	30
251	Vascular disrupting effect of CKD-516: preclinical study using DCE-MRI. Investigational New Drugs, 2013, 31, 1097-1106.	2.6	29
252	Triple Arterial Phase MR Imaging with Gadoxetic Acid Using a Combination of Contrast Enhanced Time Robust Angiography, Keyhole, and Viewsharing Techniques and Two-Dimensional Parallel Imaging in Comparison with Conventional Single Arterial Phase. Korean Journal of Radiology, 2016, 17, 522.	3.4	29

#	Article	IF	CITATIONS
253	Clinical Feasibility of Free-Breathing Dynamic T1-Weighted Imaging With Gadoxetic Acid–Enhanced Liver Magnetic Resonance Imaging Using a Combination of Variable Density Sampling and Compressed Sensing. Investigative Radiology, 2017, 52, 596-604.	6.2	29
254	Abdominal imaging findings in adult patients with Fontan circulation. Insights Into Imaging, 2018, 9, 357-367.	3.4	29
255	Comparison of MicroFlow Imaging with color and power Doppler imaging for detecting and characterizing blood flow signals in hepatocellular carcinoma. Ultrasonography, 2020, 39, 85-93.	2.3	29
256	Relationship Between Various Patterns of Transient Increased Hepatic Attenuation on CT and Portal Vein Thrombosis Related to Acute Cholecystitis. American Journal of Roentgenology, 2004, 183, 437-442.	2.2	28
257	Comparison of Renal Ablation with Monopolar Radiofrequency and Hypertonic-Saline-Augmented Bipolar Radiofrequency: In Vitro and In Vivo Experimental Studies. American Journal of Roentgenology, 2005, 184, 897-905.	2.2	28
258	Efficacy and safety of radiofrequency ablation of hepatocellular carcinoma in the hepatic dome with the CT-guided extrathoracic transhepatic approach. European Journal of Radiology, 2006, 60, 100-107.	2.6	28
259	The diagnostic value of multiplanar reconstruction on MDCT colonography for the preoperative staging of colorectal cancer. European Radiology, 2006, 16, 2284-2291.	4.5	28
260	Selection of Appropriate Liver Resection in Left Hepatolithiasis Based on Anatomic and Clinical Study. World Journal of Surgery, 2008, 32, 413-418.	1.6	28
261	High-Definition Flow Doppler Ultrasonographic Technique to Assess Hepatic Vasculature Compared With Color or Power Doppler Ultrasonography. Journal of Ultrasound in Medicine, 2008, 27, 1491-1501.	1.7	28
262	Serum Insulin-like Growth Factor-I Level Is an Independent Predictor of Recurrence and Survival in Early Hepatocellular Carcinoma: A Prospective Cohort Study. Clinical Cancer Research, 2013, 19, 4218-4227.	7.0	28
263	Radiofrequency Ablation for Intrahepatic Recurrent Hepatocellular Carcinoma: Long-Term Results and Prognostic Factors in 168 Patients with Cirrhosis. CardioVascular and Interventional Radiology, 2014, 37, 705-715.	2.0	28
264	Prediction of Local Tumor Progression after Radiofrequency Ablation (RFA) of Hepatocellular Carcinoma by Assessment of Ablative Margin Using Pre-RFA MRI and Post-RFA CT Registration. Korean Journal of Radiology, 2018, 19, 1053.	3.4	28
265	Double Low-Dose Dual-Energy Liver CT in Patients at High-Risk of HCC. Investigative Radiology, 2020, 55, 340-348.	6.2	28
266	Bipolar radiofrequency ablation in ex vivo bovine liver with the open-perfused system versus the cooled-wet system. European Radiology, 2005, 15, 759-764.	4.5	27
267	Radiofrequency Thermal Ablation in Canine Femur: Evaluation of Coagulation Necrosis Reproducibility and MRI-Histopathologic Correlation. American Journal of Roentgenology, 2005, 185, 661-667.	2.2	27
268	Diffusion-Weighted MR. Academic Radiology, 2008, 15, 593-600.	2.5	27
269	Differentiation of lipid poor angiomyolipoma from hepatocellular carcinoma on gadoxetic acid-enhanced liver MR imaging. Abdominal Imaging, 2015, 40, 531-541.	2.0	27
270	Clinical Outcomes of Radiofrequency Ablation for Early Hypovascular HCC: A Multicenter Retrospective Study. Radiology, 2018, 286, 338-349.	7.3	27

#	Article	IF	CITATIONS
271	Recommendation for terminology: Nodules without arterial phase hyperenhancement and with hepatobiliary phase hypointensity in chronic liver disease. Journal of Magnetic Resonance Imaging, 2018, 48, 1169-1171.	3.4	27
272	Fluoroscopic-guided Covered Metallic Stent Placement for Gastric Outlet Obstruction and Post-operative Gastroenterostomy Anastomotic Stricture. Clinical Radiology, 2001, 56, 560-567.	1.1	26
273	Hepatic Radiofrequency Ablation Using Multiple Probes: Ex Vivo and In Vivo Comparative Studies of Monopolar versus Multipolar Modes. Korean Journal of Radiology, 2006, 7, 106.	3.4	26
274	Percutaneous Drainage of Postoperative Abdominal Abscess with Limited Accessibility: Preexisting Surgical Drains as Alternative Access Route. Radiology, 2006, 239, 591-598.	7.3	26
275	Clinical Application of Liver MR Imaging in Wilson's Disease. Korean Journal of Radiology, 2010, 11, 665.	3.4	26
276	CT Color Mapping of the Arterial Enhancement Fraction of VX2 Carcinoma Implanted in Rabbit Liver: Comparison With Perfusion CT. American Journal of Roentgenology, 2011, 196, 102-108.	2.2	26
277	Non-Hypervascular Hypointense Nodules ≥1 cm on the Hepatobiliary Phase of Gadoxetic Acid-Enhanced Magnetic Resonance Imaging in Cirrhotic Livers. Digestive Diseases, 2014, 32, 678-689.	1.9	26
278	Switching bipolar hepatic radiofrequency ablation using internally cooled wet electrodes: comparison with consecutive monopolar and switching monopolar modes. British Journal of Radiology, 2015, 88, 20140468.	2.2	26
279	Image quality in liver CT: low-dose deep learning vs standard-dose model-based iterative reconstructions. European Radiology, 2022, 32, 2865-2874.	4.5	26
280	Saline-Enhanced Hepatic Radiofrequency Ablation Using a Perfused-Cooled Electrode: Comparison of Dual Probe Bipolar Mode with Monopolar and Single Probe Bipolar Modes. Korean Journal of Radiology, 2004, 5, 121.	3.4	25
281	Recurrence Patterns of Combined Hepatocellular-Cholangiocarcinoma on Enhanced Computed Tomography. Journal of Computer Assisted Tomography, 2007, 31, 109-115.	0.9	25
282	Assessment of hilar and extrahepatic bile duct cancer using multidetector CT: value of adding multiplanar reformations to standard axial images. European Radiology, 2007, 17, 3130-3138.	4.5	25
283	Three-Dimensional MDCT for Preoperative Local Staging of Gastric Cancer Using Gas and Water Distention Methods: A Retrospective Cohort Study. American Journal of Roentgenology, 2010, 195, 1316-1323.	2.2	25
284	Quantification of hepatic macrosteatosis in living, related liver donors using T1â€independent, T2*â€corrected chemical shift MRI. Journal of Magnetic Resonance Imaging, 2012, 36, 1124-1130.	3.4	25
285	No-Touch Radiofrequency Ablation: A Comparison of Switching Bipolar and Switching Monopolar Ablation inEx VivoBovine Liver. Korean Journal of Radiology, 2017, 18, 279.	3.4	25
286	Quantitative ultrasound radiofrequency data analysis for the assessment of hepatic steatosis using the controlled attenuation parameter as a reference standard. Ultrasonography, 2021, 40, 136-146.	2.3	25
287	Three-dimensional MDCT imaging and CT esophagography for evaluation of esophageal tumors: preliminary study. European Radiology, 2006, 16, 2418-2426.	4.5	24
288	Preoperative evaluation of hepatic arterial and portal venous anatomy using the time resolved echo-shared MR angiographic technique in living liver donors. European Radiology, 2007, 17, 1074-1080.	4.5	24

#	Article	IF	CITATIONS
289	Magnetic resonance cholangiography: comparison of two- and three-dimensional sequences for assessment of malignant biliary obstruction. European Radiology, 2008, 18, 78-86.	4.5	24
290	Differentiation of wellâ€differentiated hepatocellular carcinomas from other hepatocellular nodules in cirrhotic liver: Value of SPIOâ€enhanced MR imaging at 3.0 Tesla. Journal of Magnetic Resonance Imaging, 2009, 29, 328-335.	3.4	24
291	Monopolar Radiofrequency Ablation Using a Dual-Switching System and a Separable Clustered Electrode: Evaluation of the <i>In Vivo</i> Efficiency. Korean Journal of Radiology, 2014, 15, 235.	3.4	24
292	Comparison of Iterative Model–Based Reconstruction Versus Conventional Filtered Back Projection and Hybrid Iterative Reconstruction Techniques. Journal of Computer Assisted Tomography, 2014, 38, 859-868.	0.9	24
293	Preoperative staging of gallbladder carcinoma using biliary MR imaging. Journal of Magnetic Resonance Imaging, 2015, 41, 314-321.	3.4	24
294	Prognostic Role of Liver Stiffness Measurements Using Magnetic Resonance Elastography in Patients with Compensated Chronic Liver Disease. European Radiology, 2018, 28, 3513-3521.	4.5	24
295	How to Best Detect Portal Vein Tumor Thrombosis in Patients with Hepatocellular Carcinoma Meeting the Milan Criteria: Gadoxetic Acid-Enhanced MRI versus Contrast-Enhanced CT. Liver Cancer, 2020, 9, 293-307.	7.7	24
296	Combined Hepatocellular-Cholangiocarcinoma: Changes in the 2019 World Health Organization Histological Classification System and Potential Impact on Imaging-Based Diagnosis. Korean Journal of Radiology, 2020, 21, 1115.	3.4	24
297	Gastrointestinal Stromal Tumors of the Duodenum: CT and Barium Study Findings. American Journal of Roentgenology, 2004, 183, 415-419.	2.2	23
298	Postbiopsy Splenic Bleeding in a Dog Model: Comparison of Cauterization, Embolization, and Plugging of the Needle Tract. American Journal of Roentgenology, 2005, 185, 878-884.	2.2	23
299	Gastrointestinal stromal tumor of the stomach: preliminary results of preoperative evaluation with CT gastrography. Abdominal Imaging, 2008, 33, 255-261.	2.0	23
300	Leiomyomas in the gastric cardia: CT findings and differentiation from gastrointestinal stromal tumors. European Journal of Radiology, 2015, 84, 1694-1700.	2.6	23
301	Liver Stiffness Measured by Two-Dimensional Shear-Wave Elastography: Prognostic Value after Radiofrequency Ablation for Hepatocellular Carcinoma. Liver Cancer, 2018, 7, 65-75.	7.7	23
302	Emerging Role of Hepatobiliary Magnetic Resonance Contrast Media and Contrast-Enhanced Ultrasound for Noninvasive Diagnosis of Hepatocellular Carcinoma: Emphasis on Recent Updates in Major Guidelines. Korean Journal of Radiology, 2019, 20, 863.	3.4	23
303	CT for lymph node staging of Colon cancer: not only size but also location and number of lymph node count. Abdominal Radiology, 2021, 46, 4096-4105.	2.1	23
304	Detection of hepatocellular carcinoma: comparison of ferumoxides-enhanced and gadolinium-enhanced dynamic three-dimensional volume interpolated breath-hold MR imaging. European Radiology, 2005, 15, 140-147.	4.5	22
305	Routine intraoperative Doppler sonography in the evaluation of complications after living-related donor liver transplantation. Journal of Clinical Ultrasound, 2007, 35, 483-490.	0.8	22
306	Effects of Spatial Resolution and Tube Current on Computer-aided Detection of Polyps on CT Colonographic Images: Phantom Study. Radiology, 2008, 248, 492-503.	7.3	22

#	Article	IF	CITATIONS
307	Computer-aided image analysis of focal hepatic lesions in ultrasonography: preliminary results. Abdominal Imaging, 2009, 34, 183-191.	2.0	22
308	Microvascular Flow Imaging of Residual or Recurrent Hepatocellular Carcinoma after Transarterial Chemoembolization: Comparison with Color/Power Doppler Imaging. Korean Journal of Radiology, 2019, 20, 1114.	3.4	22
309	Wet radio-frequency ablation using multiple electrodes: comparative study of bipolar versus monopolar modes in the bovine liver. European Journal of Radiology, 2005, 54, 408-417.	2.6	21
310	Comparison of fundamental sonography, tissue-harmonic sonography, fundamental compound sonography, and tissue-harmonic compound sonography for focal hepatic lesions. European Radiology, 2006, 16, 2444-2453.	4.5	21
311	Gastric hepatoid adenocarcinoma: CT findings. Abdominal Imaging, 2007, 32, 293-298.	2.0	21
312	Primary Biliary Lymphoma Mimicking Cholangiocarcinoma: A Characteristic Feature of Discrepant CT and Direct Cholangiography Findings. Journal of Korean Medical Science, 2009, 24, 956.	2.5	21
313	Helical CT Evaluation of the Preoperative Staging of Gastric Cancer in the Remnant Stomach. American Journal of Roentgenology, 2009, 192, 902-908.	2.2	21
314	High Spatial Resolution, Respiratory-Gated, T1-Weighted Magnetic Resonance Imaging of the Liver and the Biliary Tract During the Hepatobiliary Phase of Gadoxetic Acid–Enhanced Magnetic Resonance Imaging. Journal of Computer Assisted Tomography, 2014, 38, 360-366.	0.9	21
315	Gadoxetic acid-enhanced MRI and diffusion-weighted imaging for the detection of colorectal liver metastases after neoadjuvant chemotherapy. European Radiology, 2015, 25, 2428-2436.	4.5	21
316	Dynamic contrastâ€enhanced MRI of gastric cancer: Correlation of the perfusion parameters with pathological prognostic factors. Journal of Magnetic Resonance Imaging, 2015, 41, 1608-1614.	3.4	21
317	Comparison of Knowledge-based Iterative Model Reconstruction and Hybrid Reconstruction Techniques for Liver CT Evaluation of Hypervascular Hepatocellular Carcinoma. Journal of Computer Assisted Tomography, 2016, 40, 863-871.	0.9	21
318	Prospective Validation of Intra- and Interobserver Reproducibility of a New Point Shear Wave Elastographic Technique for Assessing Liver Stiffness in Patients with Chronic Liver Disease. Korean Journal of Radiology, 2017, 18, 926.	3.4	21
319	Preoperative MDCT Assessment of Resectability in Borderline Resectable Pancreatic Cancer: Effect of Neoadjuvant Chemoradiation Therapy. American Journal of Roentgenology, 2018, 210, 1059-1065.	2.2	21
320	LI-RADS M (LR-M) criteria and reporting algorithm of v2018: diagnostic values in the assessment of primary liver cancers on gadoxetic acid-enhanced MRI. Abdominal Radiology, 2020, 45, 2440-2448.	2.1	21
321	Tumor Stiffness Measurements on MR Elastography for Single Nodular Hepatocellular Carcinomas Can Predict Tumor Recurrence After Hepatic Resection. Journal of Magnetic Resonance Imaging, 2021, 53, 587-596.	3.4	21
322	Role of Contrast-Enhanced Ultrasound as a Second-Line Diagnostic Modality in Noninvasive Diagnostic Algorithms for Hepatocellular Carcinoma. Korean Journal of Radiology, 2021, 22, 354.	3.4	21
323	Assessment of liver fibrosis using 2-dimensional shear wave elastography: a prospective study of intra- and inter-observer repeatability and comparison with point shear wave elastography. Ultrasonography, 2020, 39, 52-59.	2.3	21
324	Combined treatment of radiofrequency ablation and acetic acid injection: an in vivo feasibility study in rabbit liver. European Radiology, 2004, 14, 1303-10.	4.5	20

#	Article	IF	CITATIONS
325	MR imaging findings of early bile duct cancer. Journal of Magnetic Resonance Imaging, 2008, 28, 1466-1475.	3.4	20
326	Additional Value of SPIO-Enhanced MR Imaging for the Noninvasive Imaging Diagnosis of Hepatocellular Carcinoma in Cirrhotic Liver. Investigative Radiology, 2009, 44, 800-807.	6.2	20
327	Gadoxetic acid-enhanced MRI with MR cholangiography for the preoperative evaluation of bile duct cancer. Journal of Magnetic Resonance Imaging, 2013, 38, 138-147.	3.4	20
328	Differentiation of poorly differentiated colorectal adenocarcinomas from well- or moderately differentiated colorectal adenocarcinomas at contrast-enhanced multidetector CT. Abdominal Imaging, 2015, 40, 1-10.	2.0	20
329	Prospective Comparison of Liver Stiffness Measurements between Two Point Shear Wave Elastography Methods: Virtual Touch Quantification and Elastography Point Quantification. Korean Journal of Radiology, 2016, 17, 750.	3.4	20
330	Clinical Feasibility of Gadoxetic Acid–Enhanced Isotropic High-Resolution 3-Dimensional Magnetic Resonance Cholangiography Using an Iterative Denoising Algorithm for Evaluation of the Biliary Anatomy of Living Liver Donors. Investigative Radiology, 2019, 54, 103-109.	6.2	20
331	Comparison of guidelines for diagnosis of hepatocellular carcinoma using gadoxetic acid–enhanced MRI in transplantation candidates. European Radiology, 2020, 30, 4762-4771.	4.5	20
332	Clinical Implication of Anti-Angiogenic Effect of Regorafenib in Metastatic Colorectal Cancer. PLoS ONE, 2015, 10, e0145004.	2.5	20
333	No-touch radiofrequency ablation using multiple electrodes: An in vivo comparison study of switching monopolar versus switching bipolar modes in porcine livers. PLoS ONE, 2017, 12, e0176350.	2.5	20
334	Validation of a New Point Shear-Wave Elastography Method for Noninvasive Assessment of Liver Fibrosis: A Prospective Multicenter Study. Korean Journal of Radiology, 2019, 20, 1527.	3.4	20
335	Radiofrequency Ablation of Hepatocellular Carcinoma in Patients with Decompensated Cirrhosis: Evaluation of Therapeutic Efficacy and Safety. American Journal of Roentgenology, 2006, 186, S261-S268.	2.2	19
336	Intrahepatic Extramedullary Hematopoiesis Mimicking a Hypervascular Hepatic Neoplasm on Dynamic- and SPIO-Enhanced MRI. Korean Journal of Radiology, 2008, 9, S34.	3.4	19
337	Biliary Malignancy. Journal of Computer Assisted Tomography, 2008, 32, 362-368.	0.9	19
338	Prognostic implications of tumor vascularity and its relationship to cytokeratin 19 expression in patients with hepatocellular carcinoma. Abdominal Imaging, 2012, 37, 439-446.	2.0	19
339	Dual Switching Monopolar Radiofrequency Ablation Using a Separable Clustered Electrode: Comparison with Consecutive and Switching Monopolar Modes in <i>Ex Vivo</i> Bovine Livers. Korean Journal of Radiology, 2013, 14, 403.	3.4	19
340	Clinical Feasibility of Quantitative Ultrasound Imaging for Suspected Hepatic Steatosis: Intra- and Inter-examiner Reliability and Correlation with Controlled Attenuation Parameter. Ultrasound in Medicine and Biology, 2021, 47, 438-445.	1.5	19
341	Radiologic Evaluation and Structured Reporting Form for Extrahepatic Bile Duct Cancer: 2019 Consensus Recommendations from the Korean Society of Abdominal Radiology. Korean Journal of Radiology, 2021, 22, 41.	3.4	19
342	Switching Monopolar No-Touch Radiofrequency Ablation Using Octopus Electrodes for Small Hepatocellular Carcinoma: A Randomized Clinical Trial. Liver Cancer, 2021, 10, 72-81.	7.7	19

#	Article	IF	CITATIONS
343	Added value of 80kVp images to averaged 120kVp images in the detection of hepatocellular carcinomas in liver transplantation candidates using dual-source dual-energy MDCT: Results of JAFROC analysis. European Journal of Radiology, 2011, 80, e76-e85.	2.6	18
344	Intraductal Papillary Mucinous Neoplasms With Associated Invasive Carcinoma of the Pancreas: Imaging Findings and Diagnostic Performance of MDCT for Prediction of Prognostic Factors. American Journal of Roentgenology, 2013, 201, 565-572.	2.2	18
345	Value of MR elastography for the preoperative estimation of liver regeneration capacity in patients with hepatocellular carcinoma. Journal of Magnetic Resonance Imaging, 2017, 45, 1627-1636.	3.4	18
346	Added Value of sequentially performed gadoxetic acidâ€enhanced liver MRI for the diagnosis of small (10–19 mm) or atypical hepatic observations at contrastâ€enhanced CT: A prospective comparison. Journal of Magnetic Resonance Imaging, 2019, 49, 574-587.	3.4	18
347	No-Touch vs. Conventional Radiofrequency Ablation Using Twin Internally Cooled Wet Electrodes for Small Hepatocellular Carcinomas: A Randomized Prospective Comparative Study. Korean Journal of Radiology, 2021, 22, 1974.	3.4	18
348	Quantitative Evaluation of Hepatic Steatosis Using Advanced Imaging Techniques: Focusing on New Quantitative Ultrasound Techniques. Korean Journal of Radiology, 2022, 23, 13.	3.4	18
349	Saline-Enhanced Radiofrequency Thermal Ablation of the Lung: A Feasibility Study in Rabbits. Korean Journal of Radiology, 2002, 3, 245.	3.4	17
350	Dual-Probe Radiofrequency Ablation. Investigative Radiology, 2004, 39, 89-96.	6.2	17
351	Three-dimensional MDCT Gastrography Compared With Axial CT for the Detection of Early Gastric Cancer. Journal of Computer Assisted Tomography, 2007, 31, 741-749.	0.9	17
352	Evaluation of the Longitudinal Tumor Extent of Bile Duct Cancer. Journal of Computer Assisted Tomography, 2007, 31, 469-474.	0.9	17
353	Liver metastases on quantitative color mapping of the arterial enhancement fraction from multiphasic CT scans: Evaluation of the hemodynamic features and correlation with the chemotherapy response. European Journal of Radiology, 2011, 80, e278-e283.	2.6	17
354	Negative hepatitis B envelope antigen predicts intrahepatic recurrence in hepatitis B virusâ€related hepatocellular carcinoma after ablation therapy. Journal of Gastroenterology and Hepatology (Australia), 2011, 26, 1638-1645.	2.8	17
355	Preoperative assessment of longitudinal extent of bile duct cancers using MDCT with multiplanar reconstruction and minimum intensity projections: Comparison with MR cholangiography. European Journal of Radiology, 2012, 81, 2020-2026.	2.6	17
356	Clinical Performance of Whole-Body 18F-FDG PET/Dixon-VIBE, T1-Weighted, and T2-Weighted MRI Protocol in Colorectal Cancer. Clinical Nuclear Medicine, 2015, 40, e392-e398.	1.3	17
357	Hybrid iterative reconstruction technique for liver CT scans for image noise reduction and image quality improvement: evaluation of the optimal iterative reconstruction strengths. Radiologia Medica, 2015, 120, 259-267.	7.7	17
358	Body Diffusion-weighted MR Imaging in Oncology. Magnetic Resonance Imaging Clinics of North America, 2016, 24, 31-44.	1.1	17
359	Non-hypervascular hepatobiliary phase hypointense nodules on gadoxetic acid-enhanced MR can help determine the treatment method for HCC. European Radiology, 2019, 29, 3122-3131.	4.5	17
360	Hepatic fibrosis grading with extracellular volume fraction from iodine mapping in spectral liver CT. European Journal of Radiology, 2021, 137, 109604.	2.6	17

#	Article	IF	CITATIONS
361	Imaging diagnosis of hepatocellular carcinoma: Future directions with special emphasis on hepatobiliary magnetic resonance imaging and contrast-enhanced ultrasound. Clinical and Molecular Hepatology, 2022, 28, 362-379.	8.9	17
362	Radiofrequency ablation in the liver using two cooled-wet electrodes in the bipolar mode. European Radiology, 2005, 15, 2163-2170.	4.5	16
363	An ex-vivo experimental study on optimization of bipolar radiofrequency liver ablation using perfusion-cooled electrodes. Acta Radiologica, 2005, 46, 443-451.	1.1	16
364	Detection of Recurrent Hepatocellular Carcinoma in Cirrhotic Liver after Transcatheter Arterial Chemoembolization: Value of Quantitative Color Mapping of the Arterial Enhancement Fraction of the Liver. Korean Journal of Radiology, 2013, 14, 51.	3.4	16
365	Ultra-low Peak Voltage CT Colonography: Effect of Iterative Reconstruction Algorithms on Performance of Radiologists Who Use Anthropomorphic Colonic Phantoms. Radiology, 2014, 273, 759-771.	7.3	16
366	Liver Computed Tomography With Low Tube Voltage and Model-Based Iterative Reconstruction Algorithm for Hepatic Vessel Evaluation in Living Liver Donor Candidates. Journal of Computer Assisted Tomography, 2014, 38, 367-375.	0.9	16
367	Thermal Injury–induced Hepatic Parenchymal Hypoperfusion: Risk of Hepatocellular Carcinoma Recurrence after Radiofrequency Ablation. Radiology, 2017, 282, 880-891.	7.3	16
368	CT diagnosis of gallbladder adenomyomatosis: importance of enhancing mucosal epithelium, the "cotton ball sign― European Radiology, 2018, 28, 3573-3582.	4.5	16
369	Principles for evaluating the clinical implementation of novel digital healthcare devices. Journal of the Korean Medical Association, 2018, 61, 765.	0.3	16
370	Solid Organizing Hepatic Abscesses Mimic Hepatic Tumor. Journal of Computer Assisted Tomography, 2006, 30, 189-196.	0.9	15
371	The Association of Anisakiasis in the Ascending Colon with Sigmoid Colon Cancer: CT Colonography Findings. Korean Journal of Radiology, 2008, 9, S56.	3.4	15
372	Multiple-electrode radiofrequency ablations using Octopus® electrodes in an <i>in vivo</i> porcine liver model. British Journal of Radiology, 2012, 85, e609-e615.	2.2	15
373	Initial Performance of Radiologists and Radiology Residents in Interpreting Low-Dose (2-mSv) Appendiceal CT. American Journal of Roentgenology, 2015, 205, W594-W611.	2.2	15
374	Evaluation of Perihilar Biliary Strictures: Does DWI Provide Additional Value to Conventional MRI?. American Journal of Roentgenology, 2015, 205, 789-796.	2.2	15
375	CT and MR imaging findings of the livers in adults with Fontan palliation: an observational study. Abdominal Radiology, 2020, 45, 188-202.	2.1	15
376	Clinical Feasibility of Abbreviated Magnetic Resonance With Breath-Hold 3-Dimensional Magnetic Resonance Cholangiopancreatography for Surveillance of Pancreatic Intraductal Papillary Mucinous Neoplasm. Investigative Radiology, 2020, 55, 262-269.	6.2	15
377	Comparison of four different Shear Wave Elastography platforms according to abdominal wall thickness in liver fibrosis evaluation: a phantom study. Medical Ultrasonography, 2019, 21, 22.	0.8	15
378	Sub-classification of Advanced-Stage Hepatocellular Carcinoma: A Cohort Study Including 612 Patients Treated with Sorafenib. Cancer Research and Treatment, 2018, 50, 366-373.	3.0	15

#	Article	IF	CITATIONS
379	Impact of Reference Standard on CT, MRI, and Contrast-enhanced US LI-RADS Diagnosis of Hepatocellular Carcinoma: A Meta-Analysis. Radiology, 2022, 303, 544-545.	7.3	15
380	Optimization of Wet Radiofrequency Ablation Using a Perfused-Cooled Electrode: A Comparative Study in Ex Vivo Bovine Livers. Korean Journal of Radiology, 2004, 5, 250.	3.4	14
381	Hepatic Venous Congestion After Right-lobe Living-donor Liver Transplantation. Journal of Computer Assisted Tomography, 2007, 31, 181-187.	0.9	14
382	Magnetic resonance pancreatography: comparison of two- and three-dimensional sequences for assessment of intraductal papillary mucinous neoplasm of the pancreas. European Radiology, 2009, 19, 2163-2170.	4.5	14
383	Radiofrequency Ablation for Treating Liver Metastases from a Non-Colorectal Origin. Korean Journal of Radiology, 2011, 12, 579.	3.4	14
384	Estimation of saline-mixed tissue conductivity and ablation lesion size. Computers in Biology and Medicine, 2013, 43, 504-512.	7.0	14
385	High-resolution T1-weighted gradient echo imaging for liver MRI using parallel imaging at high-acceleration factors. Abdominal Imaging, 2014, 39, 711-721.	2.0	14
386	Heterogeneous living donor hepatic fat distribution on MRI chemical shift imaging. Annals of Surgical Treatment and Research, 2015, 89, 37.	1.0	14
387	Novel Imaging Diagnosis for Hepatocellular Carcinoma: Consensus from the 5th Asia-Pacific Primary Liver Cancer Expert Meeting (APPLE 2014). Liver Cancer, 2015, 4, 215-227.	7.7	14
388	Navigated three-dimensional T1-weighted gradient-echo sequence for gadoxetic acid liver magnetic resonance imaging in patients with limited breath-holding capacity. Abdominal Imaging, 2015, 40, 278-288.	2.0	14
389	Multiphasic Dynamic Computed Tomography Evaluation of Liver Tissue Perfusion Characteristics Using the Dual Maximum Slope Model in Patients With Cirrhosis and Hepatocellular Carcinoma. Investigative Radiology, 2016, 51, 430-434.	6.2	14
390	Health economic evaluation of Gd-EOB-DTPA MRI vs ECCM-MRI and multi-detector computed tomography in patients with suspected hepatocellular carcinoma in Thailand and South Korea. Journal of Medical Economics, 2016, 19, 759-768.	2.1	14
391	Comparison of switching bipolar ablation with multiple cooled wet electrodes and switching monopolar ablation with separable clustered electrode in treatment of small hepatocellular carcinoma: A randomized controlled trial. PLoS ONE, 2018, 13, e0192173.	2.5	14
392	Value of virtual monochromatic spectral image of dual-layer spectral detector CT with noise reduction algorithm for image quality improvement in obese simulated body phantom. BMC Medical Imaging, 2019, 19, 76.	2.7	14
393	Evaluation of the Impact of Iterative Reconstruction Algorithms on Computed Tomography Texture Features of the Liver Parenchyma Using the Filtration-Histogram Method. Korean Journal of Radiology, 2019, 20, 558.	3.4	14
394	Consensus report from the 9th International Forum for Liver Magnetic Resonance Imaging: applications of gadoxetic acid-enhanced imaging. European Radiology, 2021, 31, 5615-5628.	4.5	14
395	Intrahepatic Mass-Forming Cholangiocarcinoma: Relationship Between Computed Tomography Characteristics and Histological Subtypes. Journal of Computer Assisted Tomography, 2018, 42, 340-349.	0.9	14
396	Switching Monopolar Radiofrequency Ablation Using a Separable Cluster Electrode in Patients with Hepatocellular Carcinoma: A Prospective Study. PLoS ONE, 2016, 11, e0161980.	2.5	14

#	Article	IF	CITATIONS
397	Reproducibility of liver stiffness measurements made with two different 2-dimensional shear wave elastography systems using the comb-push technique. Ultrasonography, 2019, 38, 246-254.	2.3	14
398	Small-Bowel Obstruction in a Phantom Model of ex Vivo Porcine Intestine: Comparison of PACS Stack and Tile Modes for CT Interpretation. Radiology, 2005, 236, 867-871.	7.3	13
399	Diagnostic Performance of MDCT for Predicting Important Prognostic Factors in Pancreatic Cancer. Pancreas, 2013, 42, 1316-1322.	1.1	13
400	Differential diagnosis of benign and malignant distal biliary strictures: Value of adding diffusion-weighted imaging to conventional magnetic resonance cholangiopancreatography. Journal of Magnetic Resonance Imaging, 2014, 39, 1509-1517.	3.4	13
401	Pulmonary Nodule Detection in Patients with a Primary Malignancy Using Hybrid PET/MRI: Is There Value in Adding Contrast-Enhanced MR Imaging?. PLoS ONE, 2015, 10, e0129660.	2.5	13
402	Comparison of Multidetector CT and Gadobutrol-Enhanced MR Imaging for Evaluation of Small, Solid Pancreatic Lesions. Korean Journal of Radiology, 2016, 17, 509.	3.4	13
403	Percutaneous ethanol injection therapy is comparable to radiofrequency ablation in hepatocellular carcinoma smaller than 1.5 cm. Medicine (United States), 2016, 95, e4551.	1.0	13
404	Magnetic resonance imaging evaluation of the distal oblique bundle in the distal interosseous membrane of the forearm. BMC Musculoskeletal Disorders, 2017, 18, 47.	1.9	13
405	Additional value of contrast-enhanced ultrasonography for fusion-guided, percutaneous biopsies of focal liver lesions: prospective feasibility study. Abdominal Radiology, 2018, 43, 3279-3287.	2.1	13
406	Clinical utility of real-time ultrasound-multimodality fusion guidance for percutaneous biopsy of focal liver lesions. European Journal of Radiology, 2018, 103, 76-83.	2.6	13
407	Initial Alpha-Fetoprotein Response Predicts Prognosis in Hepatitis B-related Solitary HCC Patients After Radiofrequency Ablation. Journal of Clinical Gastroenterology, 2018, 52, e18-e26.	2.2	13
408	Prospective Validation of Repeatability of Shear Wave Dispersion Imaging for Evaluation of Non-alcoholic Fatty Liver Disease. Ultrasound in Medicine and Biology, 2019, 45, 2688-2696.	1.5	13
409	Prediction of microvascular invasion of hepatocellular carcinoma: value of volumetric iodine quantification using preoperative dual-energy computed tomography. Cancer Imaging, 2020, 20, 60.	2.8	13
410	Evaluation of LI-RADS Version 2018 Treatment Response Algorithm for Hepatocellular Carcinoma in Liver Transplant Candidates: Intraindividual Comparison between CT and Hepatobiliary Agent–enhanced MRI. Radiology, 2021, 299, 336-345.	7.3	13
411	LI-RADS Tumor in Vein at CT and Hepatobiliary MRI. Radiology, 2022, 302, 107-115.	7.3	13
412	Reduced field-of-view versus full field-of-view diffusion-weighted imaging for the evaluation of complete response to neoadjuvant chemoradiotherapy in patients with locally advanced rectal cancer. Abdominal Radiology, 2021, 46, 1468-1477.	2.1	13
413	Characterization of Focal Liver Lesions with Superparamagnetic Iron Oxide-Enhanced MR Imaging: Value of Distributional Phase T1-Weighted Imaging. Korean Journal of Radiology, 2003, 4, 9.	3.4	12
414	In Vivo Efficiency of Multipolar Radiofrequency Ablation with Two Bipolar Electrodes: A Comparative Experimental Study in Pig Kidney. Journal of Vascular and Interventional Radiology, 2007, 18, 1553-1560.	0.5	12

#	Article	IF	CITATIONS
415	Detection and characterization of focal hepatic lesions: comparative study of MDCT and gadobenate dimeglumine-enhanced MR imaging. Clinical Imaging, 2008, 32, 287-295.	1.5	12
416	Feasibility of three-dimensional virtual surgical planning in living liver donors. Abdominal Imaging, 2015, 40, 510-520.	2.0	12
417	Value of Nonrigid Registration of Pre-Procedure MR with Post-Procedure CT After Radiofrequency Ablation for Hepatocellular Carcinoma. CardioVascular and Interventional Radiology, 2017, 40, 873-883.	2.0	12
418	Percutaneous Dual-Switching Monopolar Radiofrequency Ablation Using a Separable Clustered Electrode: A Preliminary Study. Korean Journal of Radiology, 2017, 18, 799.	3.4	12
419	Magnetic resonance elastography of healthy livers at 3.0 T: Normal liver stiffness measured by SE-EPI and GRE. European Journal of Radiology, 2018, 107, 46-53.	2.6	12
420	Two-dimensional Shear Wave Elastography with Propagation Maps for the Assessment of Liver Fibrosis and Clinically Significant Portal Hypertension in Patients with Chronic Liver Disease: A Prospective Study. Academic Radiology, 2020, 27, 798-806.	2.5	12
421	Hepatobiliary phase hypointense nodule without arterial phase hyperenhancement: are they at risk of HCC recurrence after ablation or surgery? A systematic review and meta-analysis. European Radiology, 2020, 30, 1624-1633.	4.5	12
422	Diagnostic Performance of 2018 KLCA-NCC Practice Guideline for Hepatocellular Carcinoma on Gadoxetic Acid-Enhanced MRI in Patients with Chronic Hepatitis B or Cirrhosis: Comparison with LI-RADS Version 2018. Korean Journal of Radiology, 2021, 22, 1066.	3.4	12
423	Iterative Reconstruction Algorithms of Computed Tomography for the Assessment of Small Pancreatic Lesions. Journal of Computer Assisted Tomography, 2013, 37, 911-923.	0.9	11
424	Huge and recurrent undifferentiated carcinoma with osteoclast-like giant cells of the pancreas. Quantitative Imaging in Medicine and Surgery, 2018, 8, 457-460.	2.0	11
425	Comparison of monoexponential, intravoxel incoherent motion diffusion-weighted imaging and diffusion kurtosis imaging for assessment of hepatic fibrosis. Acta Radiologica, 2019, 60, 1593-1601.	1.1	11
426	How to approach pancreatic cancer after neoadjuvant treatment: assessment of resectability using multidetector CT and tumor markers. European Radiology, 2022, 32, 56-66.	4.5	11
427	Assessment of the inter-platform reproducibility of ultrasound attenuation examination in nonalcoholic fatty liver disease. Ultrasonography, 2022, 41, 355-364.	2.3	11
428	Deep learning–based image reconstruction of 40-keV virtual monoenergetic images of dual-energy CT for the assessment of hypoenhancing hepatic metastasis. European Radiology, 2022, 32, 6407-6417.	4.5	11
429	Combined Radiofrequency Ablation and Hot Saline Injection in Rabbit Liver. Investigative Radiology, 2003, 38, 725-732.	6.2	10
430	Detection of Hepatocellular Carcinoma on CT in Liver Transplant Candidates: Comparison of PACS Tile and Multisynchronized Stack Modes. American Journal of Roentgenology, 2007, 188, 1337-1342.	2.2	10
431	Adenosquamous carcinoma of the extrahepatic bile duct: clinicopathologic and radiologic features. Abdominal Imaging, 2009, 34, 217-224.	2.0	10
432	Evaluation of theIn VivoEfficiency and Safety of Hepatic Radiofrequency Ablation Using a 15-G Octopus® in Pig Liver. Korean Journal of Radiology, 2013, 14, 194.	3.4	10

#	Article	lF	CITATIONS
433	Comparison of low kVp CT and dual-energy CT for the evaluation of hypervascular hepatocellular carcinoma. Abdominal Radiology, 2021, 46, 3217-3226.	2.1	10
434	Systematic review and meta-analysis of diagnostic performance of CT imaging for assessing resectability of pancreatic ductal adenocarcinoma after neoadjuvant therapy: importance of CT criteria. Abdominal Radiology, 2021, 46, 5201-5217.	2.1	10
435	Additional values of highâ€resolution gadoxetic acidâ€enhanced MR cholangiography for evaluating the biliary anatomy of living liver donors: Comparison with <i>T</i> <sub>2</sub> â€weighted MR cholangiography and conventional gadoxetic acidâ€enhanced MR cholangiography. Journal of Magnetic Resonance Imaging, 2018, 47, 152-159.	3.4	10
436	Early quantification of the therapeutic efficacy of the vascular disrupting agent, CKD-516, using dynamic contrast-enhanced ultrasonography in rabbit VX2 liver tumors. Ultrasonography, 2014, 33, 18-25.	2.3	10
437	Combined Therapy of Radiofrequency Ablation and Ethanol Injection of Rabbit Liver: An In Vivo Feasibility Study. CardioVascular and Interventional Radiology, 2004, 27, 151-7.	2.0	9
438	A New and Simple Practical Plane Dividing Hepatic Segment 2 and 3 of the Liver: Evaluation of Its Validity. Korean Journal of Radiology, 2007, 8, 302.	3.4	9
439	Comparison Study of Different Bowel Preparation Regimens and Different Fecal-Tagging Agents on Tagging Efficacy, Patients' Compliance, and Diagnostic Performance of Computed Tomographic Colonography. Journal of Computer Assisted Tomography, 2009, 33, 657-665.	0.9	9
440	Stress (Tako-Tsubo) Cardiomyopathy Following Radiofrequency Ablation of a Liver Tumor: A Case Report. CardioVascular and Interventional Radiology, 2011, 34, 86-89.	2.0	9
441	Lymph Node Metastases from Gastric Cancer: Gadofluorine M and Gadopentetate Dimeglumine MR Imaging in a Rabbit Model. Radiology, 2012, 263, 391-400.	7.3	9
442	Metastatic testicular tumor presenting as a scrotal hydrocele: An initial manifestation of pancreatic adenocarcinoma. Oncology Letters, 2014, 7, 1793-1795.	1.8	9
443	Assessment of the association between Apgar scores and seizures in infants less than 1 year old. Seizure: the Journal of the British Epilepsy Association, 2016, 37, 48-54.	2.0	9
444	No-Touch Radiofrequency Ablation of VX2 Hepatic Tumors <i>In Vivo</i> in Rabbits: A Proof of Concept Study. Korean Journal of Radiology, 2018, 19, 1099.	3.4	9
445	Comparison of Overall Survival between Surgical Resection and Radiofrequency Ablation for Hepatitis B-Related Hepatocellular Carcinoma. Cancers, 2021, 13, 6009.	3.7	9
446	Feasibility of Application of Sensitivity Encoding to the Breath-Hold T2-Weighted Turbo Spin-Echo Sequence for Evaluation of Focal Hepatic Tumors. American Journal of Roentgenology, 2005, 184, 497-504.	2.2	8
447	Radiofrequency Renal Ablation: In Vivo Comparison of Internally Cooled, Multitined Expandable and Internally Cooled Perfusion Electrodes. Journal of Vascular and Interventional Radiology, 2006, 17, 549-556.	0.5	8
448	Differentiating Focal Eosinophilic Necrosis of the Liver From Hepatic Metastases Using Unenhanced and Portal Venous Phase Computed Tomographic Imagings. Journal of Computer Assisted Tomography, 2009, 33, 705-709.	0.9	8
449	Computer-aided polyp detection on CT colonography: Comparison of three systems in a high-risk human population. European Journal of Radiology, 2010, 75, e147-e157.	2.6	8
450	Influence of the adaptive iterative dose reduction 3D algorithm on the detectability of low-contrast lesions and radiation dose repeatability in abdominal computed tomography: a phantom study. Abdominal Imaging, 2015, 40, 1843-1852.	2.0	8

#	Article	IF	CITATIONS
451	Ultrasound-guided percutaneous portal transplantation of peripheral blood monocytes in patients with liver cirrhosis. Korean Journal of Internal Medicine, 2017, 32, 261-268.	1.7	8
452	Gastrointestinal tract complications after hepatic radiofrequency ablation: CT prediction for major complications. Abdominal Radiology, 2018, 43, 583-592.	2.1	8
453	Impact of respiratory motion on liver stiffness measurements according to different shear wave elastography techniques and region of interest methods: a phantom study. Ultrasonography, 2021, 40, 103-114.	2.3	8
454	Radiofrequency Ablation Using a Separable Clustered Electrode for the Treatment of Hepatocellular Carcinomas: A Randomized Controlled Trial of a Dual-Switching Monopolar Mode Versus a Single-Switching Monopolar Mode. Korean Journal of Radiology, 2021, 22, 179.	3.4	8
455	Ultrasound-guided transient elastography and two-dimensional shear wave elastography for assessment of liver fibrosis: emphasis on technical success and reliable measurements. Ultrasonography, 2021, 40, 217-227.	2.3	8
456	Radio-pathologic correlation of biphenotypic primary liver cancer (combined hepatocellular) Tj ETQq0 0 0 rgBT /C liver MRI. European Radiology, 2021, 31, 9479-9488.	verlock 10 4.5	0 Tf 50 547 To 8
457	Simultaneous evaluation of perfusion and morphology using CRASP MRI in hepatic fibrosis. European Radiology, 2022, 32, 34-45.	4.5	8
458	Radiofrequency ablation using internally cooled wet electrodes in bipolar mode for the treatment of recurrent hepatocellular carcinoma after locoregional treatment: A randomized prospective comparative study. PLoS ONE, 2020, 15, e0239733.	2.5	8
459	MRI of magnetically labeled mesenchymal stem cells in hepatic failure model. World Journal of Gastroenterology, 2010, 16, 5611.	3.3	8
460	Subtype Classification of Intrahepatic Cholangiocarcinoma Using Liver MR Imaging Features and Its Prognostic Value. Liver Cancer, 2022, 11, 233-246.	7.7	8
461	Perfluorobutane-enhanced ultrasonography with a Kupffer phase: improved diagnostic sensitivity for hepatocellular carcinoma. European Radiology, 2022, 32, 8507-8517.	4.5	8
462	Sonographic Features of an Intraductal Polypoid Mass. Journal of Ultrasound in Medicine, 2004, 23, 1283-1291.	1.7	7
463	State-of-the-art ultrasonography of hepatocellular carcinoma. European Journal of Radiology, 2006, 58, 177-185.	2.6	7
464	Magnetic Resonance Imaging Spectrum of Solid Pseudopapillary Neoplasm of the Pancreas. Journal of Computer Assisted Tomography, 2014, 38, 249-257.	0.9	7
465	Fat-suppressed, three-dimensional T1-weighted imaging using high-acceleration parallel acquisition and a dual-echo Dixon technique for gadoxetic acid-enhanced liver MRI at 3 T. Acta Radiologica, 2015, 56, 1454-1462.	1.1	7
466	T2* Mapping from Multi-Echo Dixon Sequence on Gadoxetic Acid-Enhanced Magnetic Resonance Imaging for the Hepatic Fat Quantification: Can It Be Used for Hepatic Function Assessment?. Korean Journal of Radiology, 2017, 18, 682.	3.4	7
467	Differential Effect of HCV Eradication and Fibrosis Grade on Hepatocellular Carcinoma and All-cause Mortality. Scientific Reports, 2018, 8, 13651.	3.3	7
468	Whole tumor ablation of locally recurred hepatocellular carcinoma including retained iodized oil after transarterial chemoembolization improves progression-free survival. European Radiology, 2019, 29, 5052-5062.	4.5	7

#	Article	IF	CITATIONS
469	Inter-platform reproducibility of liver stiffness measured with two different point shear wave elastography techniques and 2-dimensional shear wave elastography using the comb-push technique. Ultrasonography, 2019, 38, 345-354.	2.3	7
470	Deep learning-based reconstruction of virtual monoenergetic images of kVp-switching dual energy CT for evaluation of hypervascular liver lesions: Comparison with standard reconstruction technique. European Journal of Radiology, 2022, 154, 110390.	2.6	7
471	Cystic Changes in Intraabdominal Extrahepatic Metastases from Gastrointestinal Stromal Tumors Treated with Imatinib. Korean Journal of Radiology, 2004, 5, 157.	3.4	6
472	Four-dimensional volume contrast ultrasound imaging of the gallbladder compared with tissue harmonic imaging: preliminary experience. European Radiology, 2004, 14, 1657-64.	4.5	6
473	Computed Tomography Features of an Intraductal Polypoid Mass. Journal of Computer Assisted Tomography, 2006, 30, 18-24.	0.9	6
474	Detection of Small (â‰ <b>2</b> 0 mm) Pancreatic Adenocarcinoma: Histologic Grading and CT Enhancement Features. Radiology, 2012, 262, 1044-1045.	7.3	6
475	Dynamic Contrast-Enhanced MRI Using a Macromolecular MR Contrast Agent (P792): Evaluation of Antivascular Drug Effect in a Rabbit VX2 Liver Tumor Model. Korean Journal of Radiology, 2015, 16, 1029.	3.4	6
476	Comparisons between image quality and diagnostic performance of 2D- and breath-hold 3D magnetic resonance cholangiopancreatography at 3T. European Radiology, 2021, 31, 8399-8407.	4.5	6
477	Utility of Real-time CT/MRI-US Automatic Fusion System Based on Vascular Matching in Percutaneous Radiofrequency Ablation for Hepatocellular Carcinomas: A Prospective Study. CardioVascular and Interventional Radiology, 2021, 44, 1579-1596.	2.0	6
478	Assessment of the Surveillance Interval at 1 Year after Curative Treatment in Hepatocellular Carcinoma: Risk Stratification. Gut and Liver, 2018, 12, 571-582.	2.9	6
479	MR findings of renal malignant fibrous histiocytoma. European Radiology, 2003, 13, L245-L246.	4.5	5
480	Combined Radiofrequency Ablation and Acetic Acid Hypertonic Saline Solution Instillation: An In Vivo Study of Rabbit Liver. Korean Journal of Radiology, 2004, 5, 31.	3.4	5
481	Differentiating Malignant From Benign Wall Thickening in Postoperative Stomach Using Helical Computed Tomography. Journal of Computer Assisted Tomography, 2007, 31, 455-462.	0.9	5
482	Multidetector Row Computed Tomographic Gastrography Findings After Endoscopic Submucosal Dissection for Early Gastric Cancer. Journal of Computer Assisted Tomography, 2009, 33, 273-279.	0.9	5
483	Comparison of accuracy and time-efficiency of CT colonography between conventional and panoramic 3D interpretation methods: An anthropomorphic phantom study. European Journal of Radiology, 2011, 80, e68-e75.	2.6	5
484	Clinical and Duplex-Sonographic Outcomes of 1,320-nm Endovenous Laser Treatment for Saphenous Vein Incompetence. Dermatologic Surgery, 2012, 38, 1704-1709.	0.8	5
485	Evaluation of lymph node metastases: Comparison of gadofluorine Mâ€enhanced MRI and diffusionâ€weighted MRI in a rabbit VX2 rectal cancer model. Journal of Magnetic Resonance Imaging, 2012, 35, 1179-1186.	3.4	5
486	Assessing Liver Function in Liver Tumors Patients: The Performance of T1 Mapping and Residual Liver Volume on Gd-EOBDTPA-Enhanced MRI. Frontiers in Medicine, 2020, 7, 215.	2.6	5

#	Article	IF	CITATIONS
487	Intra-individual comparison of dual portal venous phases for non-invasive diagnosis of hepatocellular carcinoma at gadoxetic acid–enhanced liver MRI. European Radiology, 2021, 31, 824-833.	4.5	5
488	Additional Value of Integrated <sup>18</sup> F-FDG PET/MRI for Evaluating Biliary Tract Cancer: Comparison with Contrast-Enhanced CT. Korean Journal of Radiology, 2021, 22, 714.	3.4	5
489	LI-RADS v2018: how to appropriately use ancillary features in category adjustment from intermediate probability of malignancy (LR-3) to probably HCC (LR-4) on gadoxetic acid–enhanced MRI. European Radiology, 2022, 32, 46-55.	4.5	5
490	Disease of the Gallbladder and Biliary Tree. IDKD Springer Series, 2018, , 49-56.	0.8	5
491	Risk Factors for Hypervascularization in Hepatobiliary Phase Hypointense Nodules without Arterial Phase Hyperenhancement: A Systematic Review and Meta-analysis. Academic Radiology, 2022, 29, 198-210.	2.5	5
492	Clinicoradiological features of resected serous cystic neoplasms according to morphological subtype and preoperative tentative diagnosis: can radiological characteristics distinguish serous cystic neoplasms from other lesions?. Annals of Surgical Treatment and Research, 2020, 98, 247.	1.0	5
493	Comparison of a preoperative MR-based recurrence risk score versus the postoperative score and four clinical staging systems in hepatocellular carcinoma: a retrospective cohort study. European Radiology, 2022, 32, 7578-7589.	4.5	5
494	Intraoperative Radiofrequency Ablation Using a Loop Internally Cooled-Perfusion Electrode: In Vitro and In Vivo Experiments. Journal of Surgical Research, 2006, 131, 215-224.	1.6	4
495	Consensus Report of the Third International Forum for Liver Magnetic Resonance Imaging. Investigative Radiology, 2010, 45, S1-S10.	6.2	4
496	High-intensity Focused Ultrasound Ablation of Soft-tissue Tumors and Assessment of Treatment Response with Multiparametric Magnetic Resonance Imaging: Preliminary Study Using Rabbit VX2 Tumor Model. Journal of Medical Ultrasound, 2014, 22, 99-105.	0.4	4
497	Hepatic epithelioid hemangioendothelioma: Challenges in the preoperative diagnosis. Kaohsiung Journal of Medical Sciences, 2018, 34, 659-661.	1.9	4
498	Hepatic nontuberculous mycobacterial granulomas in patients with cancer mimicking metastases: an analysis of three cases. Quantitative Imaging in Medicine and Surgery, 2019, 9, 1126-1131.	2.0	4
499	latrogenic Arterioportal Fistula Caused by Radiofrequency Ablation of Hepatocellular Carcinoma: Clinical Course and Treatment Outcomes. Journal of Vascular and Interventional Radiology, 2020, 31, 728-736.	0.5	4
500	Comparison of the Effects of Hepatic Steatosis on Monoexponential DWI, Intravoxel Incoherent Motion Diffusion-weighted Imaging and Diffusion Kurtosis Imaging. Academic Radiology, 2021, 28, S203-S209.	2.5	4
501	Usefulness of contrast-enhanced ultrasound using perfluorobutanecontaining microbubbles as a planning for percutaneous biopsies of focal hepatic lesions: a prospective feasibility study. Medical Ultrasonography, 2019, 21, 109.	0.8	4
502	Second-look breast ultrasonography after galactography in patients with nipple discharge. Medical Ultrasonography, 2020, 1, 58.	0.8	4
503	Diagnostic Performance of Spin-Echo Echo-Planar Imaging Magnetic Resonance Elastography in 3T System for Noninvasive Assessment of Hepatic Fibrosis. Korean Journal of Radiology, 2022, 23, 180.	3.4	4
504	Multidetector CT of Extrahepatic Bile Duct Cancer: Diagnostic Performance of Tumor Resectability and Interreader Agreement. Radiology, 2022, 304, 96-105.	7.3	4

#	Article	IF	CITATIONS
505	Identifying high-risk colon cancer on CT an a radiomics signature improve radiologist's performance for T staging?. Abdominal Radiology, 2022, 47, 2739-2746.	2.1	4
506	Palliation of Malignant Gastric Obstruction: Fluoroscopic-Guided Covered Metallic Stent Placement. Journal of the Korean Radiological Society, 2000, 42, 459.	0.0	3
507	Radiologist Performance in Differentiating Polypoid Early From Advanced Gastric Cancer Using Specific CT Criteria: Emphasis on Dimpling Sign. American Journal of Roentgenology, 2009, 193, 1546-1555.	2.2	3
508	Detection and characterization of focal hepatic lesions by T2-weighted imaging: comparison of navigator-triggered turbo spin-echo, breath-hold turbo spin-echo, and HASTE sequences. Clinical Imaging, 2009, 33, 281-288.	1.5	3
509	Comparison of Semiautomated and Manual Measurements for Simulated Hypo- and Hyper-attenuating Hepatic Tumors on MDCT. Academic Radiology, 2011, 18, 626-633.	2.5	3
510	Diagnostic Value of High Frame Rate Contrast-enhanced Ultrasonography and Post-processing Contrast Vector Imaging for Evaluation of Focal Liver Lesions: A Feasibility Study. Ultrasound in Medicine and Biology, 2020, 46, 2254-2264.	1.5	3
511	Cardiovascular and abdominal flow alterations in adults with morphologic evidence of liver disease post Fontan palliation. International Journal of Cardiology, 2020, 317, 63-69.	1.7	3
512	Evaluation of Primary Liver Cancers Using Hepatocyteâ€Specific Contrastâ€Enhanced <scp>MRI</scp> : Pitfalls and Potential Tips. Journal of Magnetic Resonance Imaging, 2021, 53, 655-675.	3.4	3
513	Clinical outcomes of patients with a high alpha-fetoprotein level but without evident recurrence on CT or MRI in surveillance after curative-intent treatment for hepatocellular carcinoma. Abdominal Radiology, 2021, 46, 597-606.	2.1	3
514	Volumetric CT Texture Analysis of Intrahepatic Mass-Forming Cholangiocarcinoma for the Prediction of Postoperative Outcomes: Fully Automatic Tumor Segmentation Versus Semi-Automatic Segmentation. Korean Journal of Radiology, 2021, 22, 1797-1808.	3.4	3
515	Bronchial Arterial Embolization for Hemoptysis: Analysis of Outcome in Various Underlying Causes. Journal of the Korean Radiological Society, 1999, 41, 45.	0.0	3
516	CT Findings of Ciliated Hepatic Foregut Cyst Mimicking Metastasis: A Case Report. Journal of the Korean Radiological Society, 2000, 43, 77.	0.0	2
517	Volumetric Contrast Imaging in Bile Duct Sonography:Technology and Early Clinical Experience. American Journal of Roentgenology, 2004, 183, 1602-1604.	2.2	2
518	In vitro CT evaluation of intrahepatic stones: correlation with chemical composition. European Journal of Radiology, 2005, 54, 258-263.	2.6	2
519	Using Adobe Acrobat to Create High-Resolution Line Art Images. American Journal of Roentgenology, 2009, 193, W112-W117.	2.2	2
520	Alteration of MRP2 expression and the graft outcome after liver transplantation. Annals of Surgical Treatment and Research, 2018, 95, 249.	1.0	2
521	Can MRI Features Predict Prognosis in Mass-forming Intrahepatic Cholangiocarcinoma?. Radiology, 2019, 290, 700-701.	7.3	2
522	Detection of distant metastases in rectal cancer: contrast-enhanced CT vs whole body MRI. European Radiology, 2021, 31, 104-111.	4.5	2

#	Article	IF	CITATIONS
523	Early response evaluation of doxorubicin-nanoparticle-microbubble therapy in orthotopic hepatocellular carcinoma rat model using contrast-enhanced ultrasound and intravoxel incoherent motion-diffusion MRI. Ultrasonography, 2021, , .	2.3	2
524	Detection of Hepatic VX2 Tumors in Rabbits: Comparison of Conventional US and Phase-Inversion Harmonic US During the Liver-Specific Late Phase of Contrast Enhancement. Korean Journal of Radiology, 2003, 4, 124.	3.4	2
525	Accelerated Pancreatobiliary <scp>MRI</scp> for Pancreatic Cancer Surveillance in Patients With Pancreatic Cystic Neoplasms. Journal of Magnetic Resonance Imaging, 2022, 56, 1757-1768.	3.4	2
526	Clinical Utility of Liver Stiffness Measurements on Magnetic Resonance Elastrography in Patients with Hepatocellular Carcinoma Treated with Radiofrequency Ablation. Investigative Magnetic Resonance Imaging, 2016, 20, 231.	0.4	1
527	Comparative characteristics of quantitative indexes for 18F-FDG uptake and metabolic volume in sequentially obtained PET/MRI and PET/CT. Nuclear Medicine Communications, 2017, 38, 333-339.	1.1	1
528	FRI-485-Laparoscopic liver resection vs. Percutaneous radiofrequency ablation for small single nodular HCC: Comparison of treatment outcome. Journal of Hepatology, 2019, 70, e611-e613.	3.7	1
529	Radiofrequency Tissue Ablation with Cooled-Tip Electrodes:An Experimental Study in a Bovine Liver Model on Variables Influencing Lesion Size. Journal of the Korean Radiological Society, 2001, 44, 351.	0.0	1
530	Ultrasound-Guided Radiofrequency Thermal Ablation of Normal Kidney in a Rabbit Model: Correlation with CT and Histopathology. Journal of the Korean Radiological Society, 2002, 46, 25.	0.0	1
531	Imaging Diagnosis of Pancreatic Cancer: CT and MRI. , 2017, , 95-114.		1
532	Dual-Energy CT for Risk of Postoperative Pancreatic Fistula. Radiology, 2022, , 220320.	7.3	1
533	CT and MR Findings of Primary Hepatic Leiomyosarcoma: A Case Report. Journal of the Korean Radiological Society, 1997, 37, 1087.	0.0	0
534	Intraperitoneal Hemorrhage Due to Spontaneous Rupture of Hepatocellular Carcinoma: Comparisons of Tranarterial Oily Chemoembolization and Simple Embolization with Gelfoam. Journal of the Korean Radiological Society, 2000, 43, 171.	0.0	0
535	Hemangioma and Hepatocellular Carcinoma: Distinction with Superparamagnetic Iron Oxide-Enhanced MR Imaging. Journal of the Korean Radiological Society, 2000, 43, 195.	0.0	0
536	Superparamagnetic Iron Oxide Enhanced MR Imaging: Influence of Hepatic Dysfunction in Cirrhotic Patients. Journal of the Korean Radiological Society, 2000, 43, 319.	0.0	0
537	Excretory MR Urography Using Breathhold Three-dimensional FISP: Comparison with MR Urography Using HASTE Technique. Journal of the Korean Radiological Society, 2000, 43, 331.	0.0	0
538	Comparison of polyp distance on CT colonography between supine and prone scans using an automated path-distance measurement tool: correlation with colonoscopy. Abdominal Imaging, 2010, 35, 41-48.	2.0	0
539	Magnetic resonance cholangiopancreatography. , 0, , 123-133.		0
540	Imaging Findings of Cirrhotic Liver. Medical Radiology, 2012, , 47-83.	0.1	0

0

#	Article	IF	CITATIONS
541	Two Cases of Diabetic Ketoacidosis Associated with Paliperidone Treatment in Schizophrenia. Journal of Korean Diabetes, 2014, 15, 178.	0.3	0
542	Imaging and quantification of fatty liver by terahertz wave. , 2014, , .		0
543	Diffuse Liver Disease. Radiology Illustrated, 2014, , 21-73.	0.0	0
544	In-Service Education and Training for Teachers in Korea and the Role of the Private Sector from 1945 to 1970s. Asia-Pacific Education Researcher, 2014, 23, 413-424.	3.7	0
545	Imaging of IPMN of the pancreas: evaluation of malignant potential and resectability. Cancer Imaging, 2015, 15, .	2.8	0
546	Old and New MR Tools to Measure Hepatic Steatosis: Is Their Diagnostic Accuracy the Same?. Radiology, 2017, 284, 303-304.	7.3	0
547	Pancreatic Tumors. Medical Radiology, 2017, , 491-525.	0.1	0
548	Fluoroscopically Guided Biopsy of Intrathoracic Lesions: Diagnostic Accuracy of Combined Method Including Automated Gun Biopsy and Fine Needle Aspiration. Journal of the Korean Radiological Society, 2000, 43, 53.	0.0	0
549	SPIO-enhanced MR Imaging for HCC Detection in Cirrhotic Patient: Comparison of Various Techniques for Optimal Sequence Selection. Journal of the Korean Radiological Society, 2000, 42, 787.	0.0	0
550	Ankle Ligaments: Comparison of MR Arthrography with Conventional MR Imaging in Amputated Feet. Journal of the Korean Radiological Society, 2001, 44, 513.	0.0	0
551	Differentiation between Tuberculous and Pyogenic Spondylitis on Gd-enhanced MR Imaging: Focus on the Patterns of Disc Enhancement. Journal of the Korean Radiological Society, 2001, 45, 243.	0.0	0
552	Mn-DPDP-enhanced MR Imaging: the Optimal Pulse Sequence for Detection of Focal Hepatic Tumor. Journal of the Korean Radiological Society, 2002, 46, 367.	0.0	0
553	Usefulness of Three-dimensional Contrast-Enhanced MR Angiography in the Evaluation of Pelvic and Lower Extremity Arteries. Journal of the Korean Radiological Society, 2002, 47, 573.	0.0	0
554	Contrast-Enhanced Three-Dimensional MR Imaging Using a Volumetric Interpolated Breath-hold Examination (VIBE): Clinical Utility in the Evaluation of Renal Tumors. Journal of the Korean Radiological Society, 2002, 47, 635.	0.0	0
555	Gadobenate Dimeglumine-enhanced MR of VX2 Carcinoma in Rabbit Liver: Usefulness of the Delayed Phase Imaging and Optimal Pulse Sequence. Journal of the Korean Radiological Society, 2002, 47, 51.	0.0	0
556	The Usefulness of T2-weighted MR Urography and Contrast Enhanced MR Urography in the Evaluation of Obstructive Uropathy: Comparisonal Study with Antegrade Pyelography1. Journal of the Korean Radiological Society, 2002, 46, 49.	0.0	0
557	Preoperative Imaging of Liver Cancers: Hepatocellular Carcinoma. , 2011, , 51-59.		0

558 MR Imaging of Hepatocellular Carcinoma. , 2014, , 169-207.

#	Article	IF	CITATIONS
559	Clinical Utility of MicroPure US Imaging for Breast Microcalcifications. Journal of the Korean Society of Radiology, 0, 83, .	0.2	0
560	Neoplasms of the Gallbladder and Biliary Tract. , 2015, , 1402-1426.		0
561	Analysis of clinical phenotypes of neuropathic symptoms in patients with type 2 diabetes: A multicenter study. Journal of Diabetes Investigation, 0, , .	2.4	0